Helsinki University of Technology
Optics and Molecular Materials
Espoo 2004

ATOM TRAPS ON AN EVANESCENT-WAVE MIRROR

Andriy Shevchenko

TEKNILLINEN KORKEAKOULU
TEKNISKA HÖGSKOLAN
HELSINKI UNIVERSITY OF TECHNOLOGY
TECHNISCHE UNIVERSITÄT HELSINKI
UNIVERSITE DE TECHNOLOGIE D'HELSINKI

Helsinki University of Technology
Optics and Molecular Materials
Espoo 2004

ATOM TRAPS ON AN EVANESCENT-WAVE MIRROR

Andriy Shevchenko

Dissertation for the degree of Doctor of Science in Technology to be presented with due permission of the Department of Engineering Physics and Mathematics for public examination and debate in Auditorium F1 at Helsinki University of Technology (Espoo, Finland) on the 8th of October, 2004, at 12 noon.

Helsinki University of Technology
Department of Engineering Physics and Mathematics
Optics and Molecular Materials

Teknillinen korkeakoulu
Teknillisen fysiikan ja matematiikan osasto
Optiikka ja molekyylimateriaalit

Distribution:
Helsinki University of Technology
Optics and Molecular Materials
P.O. Box 2200
FIN-02015 HUT
Tel. +358-9-451-3153
Fax. +358-9-451-3155
Available in pdf format at http://lib.hut.fi/Diss

ISBN 951-22-7289-3

Otamedia Oy
Espoo 2004

HELSINKI UNIVERSITY OF TECHNOLOGY P.O. BOX 1000, FIN-02015 HUT http://www.hut.fi	ABSTRACT OF DOCTORAL DISSERTATION

Author Andriy Shevchenko

Name of the dissertation

ATOM TRAPS ON AN EVANESCENT-WAVE MIRROR

Date of manuscript 2.9.2004	Date of the dissertation 8.10.2004
☐ Monograph	☑ Article dissertation (summary + original articles)

Department	Department of Engineering Physics and Mathematics
Laboratory	Optics and Molecular Materials
Field of research	Laser cooling and trapping of neutral atoms
Opponent(s)	Professor Tilman Pfau
Supervisor	Professor Matti Kaivola
(Instructor)	

Abstract

During the past two decades the dramatic developments in cooling and trapping of gaseous atomic samples has produced a variety of techniques to manipulate the external and internal atomic states with electromagnetic fields. The research efforts so far have mainly focused on studying the fundamental aspects of modern quantum physics, although numerous practical applications, e.g., in integrated matter-wave optics and quantum information processing, are expected to soon be added to the already established atom-optics products, such as atomic clocks and acceleration sensors. One of the most promising foundations for the practical applications of Bose-Einstein condensates (BECs) and coherent matter waves is the technology based on the creation of microscopic atom traps on the surface of a solid substrate. This trapping technique has recently been used to successfully control the motion of microscopic atomic samples and to significantly simplify the creation of BEC.

The main research topic of this thesis is the development and design of surface-mounted atom traps on transparent dielectric substrates. Such traps could provide an extra flexibility and stability for the experiments, since they would allow unimpeded control of atoms with laser light and provide reduction of magnetic-field fluctuations associated with the thermal motion of free electrons in the substrate material. The thesis describes several novel approaches to the creation of such surface traps by superimposing repulsive evanescent optical waves with strongly localized magnetic or electric fields. These fields can be produced by either conductive or permanently magnetized, optically transparent patterns imprinted in a thin layer on a transparent dielectric substrate. The evanescent wave can also be used to cool the atoms in a gravitational field before loading them into the microtrap. The lateral confinement of the atoms on the evanescent wave can be realized with a thin-walled hollow laser beam, the creation of which is demonstrated in the thesis. The thesis also describes certain general aspects concerning evanescent-wave cooling. In particular, the influence that multiple reabsorption of resonance-frequency photons in a cloud of evanescent-wave cooled atoms has on the cooling efficiency is investigated. Also, a theoretical model based on classical statistical mechanics and thermodynamics is introduced to show how a microtrap on an evanescent-wave mirror can be used to decrease the temperature, increase the phase-space density, and provide temperature conserving spin-polarization of the atoms.

Keywords laser cooled atoms, evanescent-wave cooling, gravito-optical surface trap, microtraps

UDC	Number of pages 50
ISBN (printed) 951-22-7289-X	ISBN (pdf) 951-22-7290-3
ISBN (others)	ISSN

Publisher Helsinki University of Technology

Print distribution

☑ The dissertation can be read at http://lib.hut.fi/Diss/

Preface

The research summarized in this work has been carried out at the Optics and Molecular Materials Laboratory of Helsinki University of Technology in the Department of Engineering Physics and Mathematics in collaboration with the Metrology Research Institute of Helsinki University of Technology and Prof. J. Javanainen from the Department of Physics of University of Connecticut in USA.

I am indebted to my supervisor Prof. Matti Kaivola for his support and guidance during the course of this work, for teaching me a lot of scientific practise and providing help with manuscript preparation. I am grateful to Prof. Juha Javanainen for his invaluable contribution to this work. I thank also Pasi Ryytty, Timo Kajava, Klas Lindfors, Tero Setälä, Antti Hakola, Scott Buchter, Markus Hautakorpi, Antti Jaakkola, Thomas Lindvall, Ilkka Tittonen, and Anu Huttunen for their collaboration during my work at HUT. I am obliged to all the people (present and former) in the *Miilu* laboratory for a humorous and lively working environment. I thank our laboratory secretary Ms. Orvokki Nyberg for arranging the practical matters.

I wish to express my gratitude to the Academy of Finland for funding my doctoral studies. Personal grants from the Vilho, Yrjö and Kalle Väisälä Foundation and the Magnus Ehrnrooth Foundation are gratefully acknowledged.

I thank my parents for their continuous support, my friends, especially Victor and Maia Jeganov, for providing a nice counterbalance to my work, and, of course, special thanks to my wife Anna and son Kirill who have always been an essential part of the work I have ever done during the years of our common life.

Espoo, May 2004

Andriy Shevchenko

List of Publications

This thesis is a review of the author's work on development of novel methods for manipulation of neutral atoms using surface-mounted microscopic atom traps. It consists of an overview and the following selection of the author's publications in the field:

I. A. Shevchenko, S. C. Buchter, N. V. Tabiryan, and M. Kaivola, "Creation of a hollow laser beam using self-phase modulation in a nematic liquid crystal", *Opt. Commun.* **232**, 77 (2004).

II. A. Shevchenko, J. Javanainen, and M. Kaivola, "Heating and phase-space decompression of evanescent-wave cooled atoms by multiple photon reabsorption", *Opt. Exp.* **11**, 1827 (2003).

III. A. Shevchenko, T. Lindvall, I. Tittonen, and M. Kaivola, "Microscopic electro-optical atom trap on an evanescent-wave mirror", *Eur. Phys. J. D* **28**, 273 (2004).

IV. A. Shevchenko, A. Jaakkola, T. Lindvall, I. Tittonen, and M. Kaivola, "Method for obtaining high phase-space density in a surface-mounted atom trap", *Appl. Phys. B* **79**, 367 (2004).

V. A. Shevchenko, J. Javanainen, and M. Kaivola, "Thermodynamics of a multi-component-atom sample in a tightly compressed atom trap", *Phys. Rev. A* **70**, 011403 (R) (2004).

Throughout the overview, these papers will be referred to by Roman numerals.

Author's Contribution

The research presented in this dissertation is the result of the work on development of surface-mounted microscopic atom traps and guides carried out during the years 2001–2004 in the Optics and Molecular Materials Laboratory of Helsinki University of Technology in collaboration with the Metrology Research Institute of Helsinki University of Technology and Prof. J. Javanainen from the Department of Physics of University of Connecticut in USA.

The author has played a central role in all aspects of the research work. He has implemented all the experimental and theoretical work in paper I. He has developed a theoretical method and performed the calculations in paper II. He is the author of the ideas reported in papers III and IV. The study leading to paper V has been initiated and conducted by the author, with a theoretical approach and numerical methods being proposed by Prof. J. Javanainen. All the papers were written by the author.

Other publications by the author or to which the author has contributed:

- A. Shevchenko, P. Ryytty, T. Kajava, M. Hautakorpi, and M. Kaivola, "Single-longitudinal-mode selection in a nanosecond-pulsed dye laser", *Appl. Phys. B* **74**, 349 (2002).
- T. Setälä, A. Shevchenko, M. Kaivola, and A. T. Friberg, "Degree of polarization for optical near fields", *Phys. Rev. E* **66**, 016615 (2002).
- A. Shevchenko, S. C. Buchter, N. V. Tabiryan, and M. Kaivola, "Self-focusing in a nematic liquid crystal for measurements of wavefront distortions", *Opt. Commun.* **232**, 439 (2004).
- M. Hautakorpi, A. Shevchenko, and M. Kaivola, "Spatially smooth evanescent-wave profiles in a multimode hollow optical fiber for atom guiding", *Opt. Commun.* **237**, 103 (2004).

Contents

1 Introduction

When the thermal motion of atoms and molecules becomes slower, a variety of quantum-mechanical phenomena, such as superconductivity and superfluidity, become available for investigation and use. Whereas ordinary cryogenic methods provide cooling to temperatures in the range from a few K down to about 100 mK, laser cooling of gaseous atomic samples moves the temperature limit below 1 μK. At these temperatures, the de Broglie wavelength of the atoms is so large that operations and tasks familiar from ordinary light-wave optics can be performed using atomic matter waves. Research work on laser cooling and trapping started in the 1970s. By the end of the 1980s, there had been an explosion of interest in this field that culminated in the award of the Nobel Prize in Physics in 1997. Shortly after this, in December of 2001, the Nobel Prize was again awarded to researchers in this field for the achievement of Bose-Einstein condensation (BEC), which has been the most significant and spectacular application of laser cooling and trapping so far.

The first steps in the manipulation of the *internal* degrees of freedom of atoms and molecules with an electromagnetic field were taken by I. I. Rabi, who, in 1938, introduced an apparatus to coherently control the magnetic states of particles with radio-frequency radiation [1]. Rabi's atomic-beam method was further developed in 1949 by N. Ramsey to allow the use of quantum interference between two internal atomic states [2]. The invention of this first atom interferometer formed the basis for atomic clocks with extraordinary precision and accuracy. Extension of Ramsey's method to the optical domain would provide improvement of the accuracy by several orders of magnitude. However, fruitful experiments in this direction could start only in the 1970s with the development of narrow-band tunable lasers [3, 4].

In regard to manipulation of the *external* degrees of freedom of atoms, the 70's were a turning point, as laser radiation was shown to be an efficient means to deflect [5–7], diffract [8, 9], as well as trap [10–12] and cool [13–16] neutral atoms. The research work initiated by these first results eventually led to the invention of the magneto-optical trap (MOT) [17], which is nowadays the most widely used tool for trapping and cooling atoms. In 1995, by using a MOT and applying the evaporative cooling, first described by H. F. Hess in 1986 [18], Bose-Einstein condensation of a gas of ^{87}Rb was for the first time observed in an experiment [19]. This new state of matter, predicted 70 years ago by Bose and Einstein, had become a part of reality. This event resulted in an explosion of research activity in the field of quantum-degenerate gases. BECs of ^{23}Na [20] and ^{7}Li [21] were obtained in the same year. Afterward, in 1998 atomic hydrogen [22], in 2000 ^{85}Rb [23], in 2001 ^{41}K [24] and metastable ^{4}He [25], and in 2003 ^{133}Cs [26] were added to the list of Bose-condensed atoms. Molecular condensates have also been obtained quite recently [27–29]. Studying the unique properties of condensed Bose gases, such as superfluidity [30–34], phase transition from superfluid to Mott insulator [35],

formation of solitons [36, 37] and vortices [38–41], matter-wave mixing [42–44] and amplification [45,46], as well as atom lasing [47–49] is today in rapid progress. Also, degenerate Fermi gases of ^{6}Li and ^{40}K have been experimentally realized during the past few years, and a large effort is directed towards achievement of Cooper pairing and superfluidity in these gases [27–29, 50–57].

As the invention of the optical laser led to development of entirely new ways to create and manipulate photons, the achievement of BEC opened up perspectives for the development of new technology for the creation and manipulation of coherent matter waves. Condensed atoms, characterized by the same wave function and the same phase, retain memory of their initial state after they are released out of the trap. The deep analogy of light and matter, framed by their common particle-wave dualism, allows one to use light optics foundations as building blocks for novel experiments of *atom optics* with the waves of matter. In contrast to photons, however, atoms have mass, and, in addition, they directly interact with each other. The interaction strength and sign can be magnetically tuned by using Feshbach resonances [58,59]. Moreover, as an electromagnetic field can be manipulated with material objects composed of atoms, atoms can be manipulated with electromagnetic fields. These properties, together with the possibility to employ internal atomic states, enable atom optics to find a rich variety of unique applications in science and technology.

Creation of BEC with today's standard methods is unfortunately still technically difficult and an experimentally delicate task. Therefore, invention and development of less complicated and more flexible methods is of particular interest. One of the most likely foundations for practical applications of atom optics and Bose-Einstein condensation is the technique based on trapping atoms in surface-mounted microscopic traps above lithographically fabricated current-carrying wires [60, 61]. Well-localized magnetic [61–63] or electric [64, 65] fields above the surface of a room-temperature solid substrate have been successfully used to control the motion of microscopic atomic samples [61, 64], and to essentially simplify the creation of BEC [61, 66, 67]. In view of providing further flexibility to the control and manipulation of atoms, microfabrication techniques make it possible to integrate many atom-optical elements, such as microtraps [68,69], waveguides [69–71], beam splitters [72,73], and interferometers [74–76], on a single "atom chip". The research on development of miniaturized atom-optical devices includes searching and realization of new ideas, such as trapping of atoms with the aid of microscopic permanent magnets [77–79] and creation of all-optical atom traps and guides by using microlens arrays [80–82]. Also, the theory describing atoms in surface-mounted traps [75, 76, 83–85], with many far-reaching proposals for future applications including fundamental studies of low-dimensional condensates [86–90] and Tonks gases [91, 92], cavity quantum electrodynamics [93, 94], and quantum information processing [85, 95] is in continuous development.

The main goal of this thesis is to introduce our first steps in the development of novel technique for manipulation of microscopic atom samples by making use of evanescent optical fields. In particular, we study the possibility to realize an atom chip on a substrate which is transparent to light. This feature could add flexibility to laser control of both the internal and external states of the atoms. One of the benefits of this approach lies in the possibility to efficiently cool atoms directly on the surface by using a gravito-optical surface trap (GOST) [96–98]. The atoms in the GOST are cooled by inelastic reflections from the evanescent wave, which finally results in the formation of an atom cloud with a thermal height of a few tens of μm above the surface. The atoms can then be loaded into a surface-mounted microtrap by the process of equilibration of atom density after inserting the microtrap into the GOST. Since the microtrap is small in volume, the temperature remains low. Owing to this, the phase-space density in the microtrap can reach a level of $10^{-2} - 10^{-1}$, which by far exceeds the values achieved in loading of conventional traps on a chip. The high phase-space density should be a good starting point for creating, e.g., Bose-Einstein condensates. A BEC of ^{133}Cs on a prism surface has recently been obtained, using a GOST and an all-optical subtrap [99]. By fabricating microscopic wires or electrodes, as well as permanently magnetized structures, of transparent materials one can realize an atom-chip design with an easily applied optical, magnetic, and static-electric field control of the atomic motion. In this thesis, we describe several approaches to the creation of microscopic atom traps mounted on a surface and discuss the methods which can provide efficient cooling, strong phase-space compression, and temperature conserving spin-polarization of the atoms by using an adiabatically driven deformation of the trapping potential. In addition, we note that in such optically transparent devices, the quantum states of the atoms can readily be manipulated and probed using laser light.

The thesis consists of five sections. In section 2, we briefly describe the main aspects of the atom-field interaction theory in the context of its applications to atom cooling and trapping. Section 3 describes the basics of trapping and cooling of atoms on an evanescent optical wave. Section 4 is mainly devoted to creation of microscopic atom traps on an evanescent-wave mirror and to a method of loading of these traps with atoms. It also introduces a theoretical description of a multicomponent atom sample in a trap containing an adiabatically inserted or removed subtrap. The main results of the work are summarized in section 5.

2 Atoms in electromagnetic fields

A free atom is characterized by a fixed set of allowed internal quantum states dictated by the structure of its nucleus and the number of its electrons. The interaction of the atom with an electromagnetic field can be described in terms of transitions of the atom between these states, including their linear superpositions, as well as the field-induced shifts and broadenings of the atomic energy levels. The transitions obey the laws of conservation of energy and momentum. Conservation of linear momentum, for example, plays an essential role in laser cooling, and that of angular momentum in optical pumping. The forces experienced by atoms due to their interaction with an electromagnetic field are dissipative, if the mechanisms involve spontaneous relaxation of atoms from excited states. Spatially inhomogeneous shifts of atomic energy levels, such as the light shift, the static Stark shift, and the Zeeman shift, lead to conservative forces, which can be employed in atom trapping and in certain cooling mechanisms, such as the so-called Sisyphus cooling.

While ions have a strong coupling of their charge to static electric and magnetic fields, neutral atoms interact with these fields only weakly by field-induced electric dipole moments (static Stark effect) or permanent magnetic moments (Zeeman effect). The *dipole* moments of atoms in a static electric field depend on the zero-frequency polarizability of the atoms. For alkali atoms in the ground state, the polarizability has a value on the order of 10^{-35} C·cm^2/V, which requires electric fields of about 10 kV/cm to create a potential well of 1 mK depth. This makes it technically inconvenient to use the static Stark effect for trapping atoms. On the other hand, if atoms are trapped close to a thin charged wire or to a small gap between two oppositely charged electrodes, the electric potential can be made deep with a low-voltage source [60, 100, 101]. For realization of comparable interaction potentials, the coupling of the *magnetic* moments of atoms (μ) to a static magnetic field is stronger. The values of μ are on the order of the Bohr magneton, $\mu_B \approx 9.3 \times 10^{-20}$ A·cm^2, and a 1 mK deep well is obtained by applying a magnetic field of a few tens of Gauss.

Although a static electric potential always attracts atoms to a high-field region, the magnetic potential can be either attractive (for atoms in a state with $\mu > 0$) or repulsive ($\mu < 0$). The latter allows creating purely magnetic traps in free space. A local *maximum* of both static electric and magnetic fields in a charge-free space is forbidden. These properties of the atom-field interaction make magnetic traps more popular, although in some applications, where atoms should be confined independently of their spins, the use of electric fields can be superior.

The action of an *optical* field on atoms depends on the field frequency and intensity. The interaction effects become stronger when the frequency approaches a resonance frequency of the atoms and when the light intensity increases. The interaction is usually accompanied by absorption of photons and either spontaneous

or stimulated emission. Each of these transitions leads to a change of momentum of the atom by the momentum of the photon. In the presence of spontaneous emission, atoms experience the so-called *radiation pressure force*. This force is related to the momentum transfer in the absorption events, since the average momentum of spontaneously emitted photons is zero. Another force, the so-called *dipole force*, is associated with virtual transitions or, in the dressed atom picture, with the above mentioned light shifts of the atomic energy levels. The shift of a ground-state level has the same sign as the frequency detuning, δ, of the field from the atomic resonance. The direction of the force is parallel, if $\delta < 0$, or antiparallel, if $\delta > 0$, to the spatial intensity gradient of the field. In the first case, the field is said to be *red-detuned*. It attracts atoms to the high-intensity regions. In the second case the field is *blue-detuned*, and it is repulsive for the atoms. Although blue-detuned dipole traps are more difficult to realize, they allow reduction of the mean rate of optical transitions in the trap and, as a result, are less prone to light-induced heating and loss.

In the following, we present a brief overview of the atom-field interaction theory providing a quantitative description of the effects discussed above and used in the present work.

2.1 Two-level atom and dressed atom states

The interaction of an atom with an electromagnetic field is generally described by the time-dependent Schrödinger equation,

$$i\hbar\frac{\partial}{\partial t}\Psi(\vec{r},t) = \mathcal{H}\Psi(\vec{r},t), \tag{1}$$

where $\mathcal{H} \equiv \mathcal{H}_0 + \mathcal{H}'(t)$ is the Hamiltonian of the atom in the field divided into the time-independent part $\mathcal{H}_0$ and the interaction part $\mathcal{H}'(t)$. The solution $\Psi(\vec{r},t)$ can be expanded in terms of the eigenfunctions $\phi_n(r)$ of $\mathcal{H}_0$ as

$$\Psi(\vec{r},t) = \sum_k c_k(t)\phi_k(r)e^{-iw_k t}. \tag{2}$$

The eigenvalues of $\mathcal{H}_0$ are $E_n = \hbar w_n$. Equation (1) can be rewritten in an equivalent form as

$$i\hbar\dot{c}_j(t) = \sum_k c_k(t)\mathcal{H}'_{jk}(t)e^{iw_{jk}t}, \tag{3}$$

where $\mathcal{H}'_{jk}(t) \equiv \langle\phi_j|\mathcal{H}'(t)|\phi_k\rangle$ and $w_{jk} \equiv w_j - w_k$, and where the dot denotes the total time derivative. To solve Eq. (3) for an atom initially in the ground state [$c_1(0) = 1$], one may apply perturbation theory, choosing $|c_k(t)| \ll 1$ for all k except for the lowest level $k = 1$. However, if the probability to find an atom

in an excited state can reach a high value, as in the case of interaction with an intense, nearly resonant laser light, this approach is not suitable. The two-level atom picture [102] may then be a fruitful theoretical tool. In this picture, the summation in Eq. (3) is truncated to just two terms corresponding to the states coupled by laser light. Labelling them with subindices g (ground state) and e (excited state), one obtains

$$i\hbar\dot{c}_g(t) = c_e(t)\mathcal{H}'_{ge}(t)e^{-iw_at}, \quad (4)$$
$$i\hbar\dot{c}_e(t) = c_g(t)\mathcal{H}'^{*}_{ge}(t)e^{iw_at}, \quad (5)$$

where $w_a \equiv w_{eg}$. Then, the coupling element $\mathcal{H}'_{ge}(t)$ of the interaction Hamiltonian may be written in terms of the Rabi frequency, $\Omega \equiv -\mathrm{e}\mathcal{E}_0\langle e|r|g\rangle/\hbar$, as $\mathcal{H}'_{ge}(t) = \hbar\Omega\cos(kz_c - w_lt)$, where the electric dipole approximation has been applied to the atom-field interaction $[\mathcal{H}'(t) = -\mathrm{e}\vec{\mathcal{E}}(\vec{r_c}, t)\cdot\vec{r}]$ and the plane wave approximation to the field ($\vec{r}$ is the electron coordinate and $\vec{r_c}$ is the coordinate of the atomic center of mass; $\mathcal{E}_0$ is the field amplitude and w_l the frequency). Using this Hamiltonian and applying the rotating wave approximation (valid for $\delta \equiv w_l - w_a << w_l$), one can write Eqs. (4) and (5) in the following form

$$\ddot{c}_g(t) - i\delta\dot{c}_g(t) + (\Omega^2/4)c_g(t) = 0, \quad (6)$$
$$\ddot{c}_e(t) + i\delta\dot{c}_e(t) + (\Omega^2/4)c_e(t) = 0. \quad (7)$$

The solution of these equations with the initial condition $c_g(0) = 1$ is

$$c_g(t) = [\cos(\Omega' t/2) - i(\delta/\Omega')\sin(\Omega' t/2)]\, e^{i\delta t/2}, \quad (8)$$
$$c_e(t) = -i(\Omega/\Omega')\sin(\Omega' t/2)e^{-i\delta t/2}, \quad (9)$$

where $\Omega' \equiv \sqrt{\Omega^2 + \delta^2}$. According to Eqs. (8) and (9), the probabilities $|c_g(t)|^2$ and $|c_e(t)|^2$ oscillate at frequency Ω'. This oscillation indicates a deterministic (coherent) interaction of atom with light, where the absorption and stimulated emission are fully correlated and the atom evolves through the superposition states. In particular, when $\delta = 0$, the oscillation amplitude of $|c_e(t)|^2$ is 1. Hence, all atoms in the sample can be simultaneously excited with a laser pulse of a width τ that satisfies $\Omega\tau = \pi$.

In practice, the coherent oscillation of the eigenstate probabilities is disturbed by spontaneous emission. Spontaneous emission is induced by electromagnetic fluctuations of the vacuum. In almost all cases, the number of modes carrying the vacuum "photons" is enormous, and spontaneous emission is essentially uncontrollable. The spontaneous decay rate, Γ, is therefore a stable characteristic of the state. In the dipole approximation, it reads

$$\Gamma = \frac{w_a^3\mu^2}{3\pi\epsilon_0\hbar c^3}, \quad (10)$$

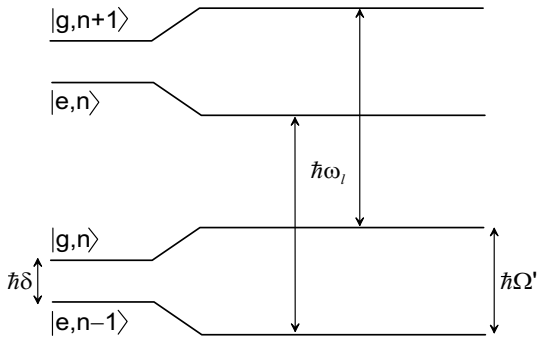

Figure 1: Energy level diagram for an atom-field system. The first and second symbols in the kets denote the state of the atom and the quantum number of the field, respectively. When the light intensity is increased, the two nearly degenerate energy levels become split by $\hbar\Omega'$ which in a fully quantum description becomes a function of n. The detuning δ in this example is positive.

where $\vec{\mu} = \mathrm{e}\langle e|\vec{r}|g\rangle$ is the dipole moment of the transition. Due to spontaneous emission, the probability oscillations of individual atoms in an atomic sample become out of phase, which results in a damping of the corresponding oscillation of the atomic energy levels' populations. The populations approach their steady-state values in a time of a few $\tau_{sp} = 1/\Gamma$ [103].

For atoms in an optical field, the eigenvalues of the total Hamiltonian $\mathcal{H}$ are shifted from the eigenvalues of the unperturbed Hamiltonian $\mathcal{H}_0$. In the rotating wave approximation the interaction Hamiltonian $\mathcal{H}'$ can be made time-independent. It can then be diagonalized to find the eigenvalues $E_{g,e} = \hbar(-\delta \pm \Omega')/2$. The corresponding energy levels are separated by $\hbar\Omega'$. The related states are called the dressed states. When the light intensity approaches zero, the energies become $E_g \approx 0$ and $E_e \approx -\hbar\delta$. The light shifts are therefore

$$\Delta E_{g,e} = \hbar(\mp\delta \pm \Omega')/2, \tag{11}$$

and in the limit of low intensity and large detuning ($\Omega \ll |\delta|$), they become

$$\Delta E_{g,e} \approx \pm\hbar\Omega^2/(4\delta). \tag{12}$$

Figure 1 shows an energy level diagram for an atom-field system, for which the total Hamiltonian is written in the form $\mathcal{H} = \mathcal{H}_0 + \mathcal{H}_{rad} + \mathcal{H}'$, where $\mathcal{H}_{rad}$ is the radiation part having the eigenvalues $E_n = \hbar w_l(1/2+n)$ and $\mathcal{H}'$ is written as above in the semiclassical approximation. The light-shifted energy levels of each dressed atom state are in this picture separated by the photon energy $\hbar w_l$.

The Rabi frequency depends on light intensity. So do the light shifts of atomic ground states (see Fig. 1). Thus, a red- or blue-detuned laser field can be used to

produce a potential well or barrier, respectively, for the atoms. The force acting on the atom (the dipole force) is proportional to the gradient of the light shift. In the case of large detuning and low intensity, the force can be written as

$$(\vec{F}_{dip})_{g,e} = \mp\frac{\hbar}{4\delta}\nabla_{\vec{r}_c}(\Omega^2), \tag{13}$$

where Eq. (12) has been applied.

2.2 Power broadening and saturation

In the calculations of section 2.1, the effect of spontaneous emission was omitted, and the atom-field interaction was described in terms of coherent evolution of the atomic states. In this section we recall the density matrix formalism and, by employing the optical Bloch equations (OBEs), describe the power broadening and saturation effects, which both are influenced by spontaneous emission [103, 104]. For a two-level system, the density matrix is

$$\rho = \begin{pmatrix} \rho_{ee} & \rho_{eg} \\ \rho_{ge} & \rho_{gg} \end{pmatrix}, \tag{14}$$

where ρ_{ee} and ρ_{gg} are the populations of the excited and ground state, respectively, and ρ_{eg} and ρ_{ge} the atomic coherence terms. Starting from the equation of motion for the density matrix, $i\hbar\dot{\rho} = [\mathcal{H}, \rho]$, and including the effects of light coupling and spontaneous emission, one can come to the OBEs in the form

$$\begin{aligned}
\dot{\rho}_{ee} &= -\Gamma\rho_{ee} - i(\Omega^*\tilde{\rho}_{eg} - \Omega\tilde{\rho}_{ge})/2, && (15)\\
\dot{\rho}_{gg} &= -\dot{\rho}_{ee}, && (16)\\
\dot{\tilde{\rho}}_{ge} &= -(\Gamma/2 + i\delta)\tilde{\rho}_{ge} + i\Omega^*(\rho_{ee} - \rho_{gg})/2, && (17)\\
\dot{\tilde{\rho}}_{eg} &= -(\Gamma/2 - i\delta)\tilde{\rho}_{eg} - i\Omega(\rho_{ee} - \rho_{gg})/2, && (18)
\end{aligned}$$

where $\tilde{\rho}_{ij} \equiv \rho_{ij}e^{i\delta t}$. A steady-state solution of these equations is found by setting all time derivatives to zero. With $\rho_{eg} = \rho^*_{ge}$, this finally yields

$$\begin{aligned}
p &= 1/(1+S) \text{ and} && (19)\\
\rho_{eg} &= \frac{i\Omega}{2(\Gamma/2 - i\delta)(1+S)}, && (20)
\end{aligned}$$

where $p \equiv \rho_{gg} - \rho_{ee}$ is the population difference and the saturation parameter S is defined by

$$S = \frac{S_0}{1 + (2\delta/\Gamma)^2}. \tag{21}$$

The parameter $S_0 \equiv 2|\Omega|^2/\Gamma^2$ is the on-resonance saturation parameter, often written as the ratio I/I_s of the light intensity I to the saturation intensity $I_s \equiv 2\pi^2\hbar c\Gamma/3\lambda^3$.

The excited-state population, ρ_{ee}, decays due to spontaneous emission at a rate of Γ. Since in the steady state, the excitation and decay rates are equal, the scattering rate of light from the laser field is $\gamma_s = \Gamma\rho_{ee}$. Taking into account the fact that $\rho_{ee} = (1 - p)/2$, one obtains

$$\gamma_s = \frac{\Gamma S}{2(1+S)} = \frac{S_0\Gamma/2}{1 + S_0 + (2\delta/\Gamma)^2}. \tag{22}$$

If S_0 increases, the scattering rate γ_s becomes less dependent on the detuning δ. As a result, the transition linewidth broadens. This is called power broadening of the transition. At high intensities and small detunings, the rate γ_s saturates to $\Gamma/2$.

Once γ_s is known, calculation of the *radiation pressure force* is straightforward, i.e.,

$$F_{rad} = \hbar k\gamma_s, \tag{23}$$

where k is the field's wavenumber. The total force found in the OBE formalism includes also the *dipole force*, $F_{dip} = \hbar\zeta_{re}(\Omega\rho^*_{eg} + \Omega^*\rho_{eg})$, where ζ_{re} is equal to $\mathrm{Re}[(1/\Omega)\partial\Omega/\partial \mathrm{z_c}]$ and the axis z is chosen to point in the direction of the force. By applying Eq. (20) one obtains $F_{dip} = -\hbar\delta\zeta_{re}S/(1+S)$. This result can be written explicitly in terms of δ and $S_0 \equiv I/I_s$, when assuming Ω to be real, as

$$F_{dip} = -\frac{\hbar\delta/2}{1 + S_0 + (2\delta/\Gamma)^2}\frac{\partial S_0}{\partial z_c}. \tag{24}$$

At low intensity and large detuning, Eq. (24) reduces to the force $(F_{dip})_g$ of Eq. (13).

2.3 Multilevel atoms

The theory described in sections 2.1 and 2.2 provides a good qualitative and often also quantitative description of the atom-field interaction for many applications of laser cooling and trapping. However, real atoms have a complex structure of their energy levels, and in general optical fields couple more than just two of them. As the present work deals with alkali atoms, we start with a brief description of their properties.

Alkali atoms have only one valence electron. The state of this electron is determined by the orbital angular momentum $\vec{l}$ and spin $\vec{s}$. Other electrons are in closed shells and their influence on the atomic states is negligible. Hence, the quantum numbers for the atom's electrons, L, S, and J, coincide with those of the valence electron, $L = l, S = s$, and $J = j$. The total angular momentum J takes the values from $|L - S|$ to $L + S$. The energy splitting (each L-level splits into $2S + 1$ levels)

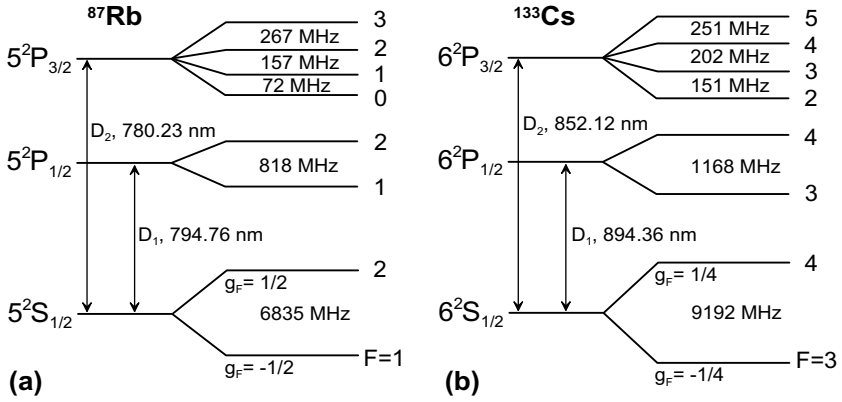

Figure 2: Fine and hyperfine structures of (a) ^{87}Rb and (b) ^{133}Cs. For ^{87}Rb the nuclear spin is $I = 3/2$, and for ^{133}Cs it is $I = 7/2$.

caused by the spin-orbit interaction forms the atomic *fine* structure, of which the states are usually specified as $n^{2S+1}L_J$ with n being the principal quantum number of the electron. The coupling between $\vec{J}$ and the nuclear spin $\vec{I}$ leads to an additional *hyperfine* splitting of the levels, since the total angular momentum of the atom, $\vec{F}$, has $2J + 1$ projections on the quantization axis (the quantum number F takes the values from $|I - J|$ to $I + J$). Examples illustrating the fine and hyperfine structures of ^{87}Rb and ^{133}Cs are shown in Fig. 2.

Each hyperfine energy level is $2F + 1$-fold degenerate. Application of a weak external magnetic field lifts this degeneracy through the anomalous Zeeman effect. The magnetic quantum number m_F, which is the projection of $\vec{F}$ on the direction of the magnetic field, runs from $-F$ to F. For weak fields, typically weaker or on the order of 10^2 Gauss, the splitting grows linearly with the field strength B and can be described by

$$\Delta E_{m_F} = \mu_B g_F m_F B, \tag{25}$$

where g_F is the Landé g-factor that accounts for the contribution of both the valence electron and nucleus, $g_F = g_J[F(F+1) + J(J+1) - I(I+1)]/[2F(F+1)]$. The g_J-factor does not depend on I and, for all alkali atoms in the ground state, it is $g_J = 2$. The g_F factors for the hyperfine ground states of ^{87}Rb and ^{133}Cs are given in Fig. 2. When the magnetic field increases above a certain value, the vectors $\vec{J}$ and $\vec{I}$ become more strongly coupled to the field than to each other. Equation (25) in this case does not hold.

Alkali atoms are normally composed of an even number of fermions (neutrons, protons, and electrons). As a result, they behave like bosons. Some isotopes of these atoms, however, have an odd number of fermions and behave like fermions. Examples of such isotopes are ^{6}Li and ^{40}K which have been recently used to create

quantum-degenerate Fermi gases and molecular BECs [27–29, 50–57].

In laser cooling and trapping, the frequencies of the D_1 and D_2 transitions (see Fig. 2) are the usual reference points for selecting the laser frequency. However, the laser bandwidth is usually much narrower than the ground-state hyperfine splitting and often narrower than the Zeeman splitting. Thus, the laser frequency has to be further specified with respect to these sublevels. When the laser is far detuned from some particular atomic resonance, or its bandwidth is large, more than one atomic transition can occur with a comparable probability. Furthermore, spontaneous emission can drive atoms to different hyperfine ground states. In many atom-optical applications, a key role belongs to the *selection rules*, such as $\Delta m_F = 0$ for transitions in linearly polarized light and $\Delta m_F = +1$ and -1 for transitions in σ^+- and σ^--polarized light, respectively. These rules are applied, e.g., in optical spin-polarizing, where in order to pump atoms into a magnetic state of a higher/lower value of m_F, one uses σ^+-/σ^--polarized light. Other selection rules, such as $\Delta L = \pm 1$ and $\Delta F = 0, \pm 1$ with the transitions $F = 0 \rightarrow F' = 0$ being forbidden, are as well frequently employed in building experiments. For example, an atomic sample in a monochromatic field that drives the D_2 transitions between either the lowest or the highest hyperfine states can be considered to be a closed two-level system, since spontaneous emission to the other levels is forbidden ($|\Delta F| = 2$ or $\Delta L = 0$). Hence, one can directly use the results of the two-level atom approximation described in section 2.1.

If more than one transition of an atom from its initial state is allowed, as in the case of spontaneous emission from, e.g., the $^2P_{1/2}$ state, the probabilities for each transition can be calculated by taking into account the relative transition strengths. For all transitions between the hyperfine energy levels of the states $^2S_{1/2}$, $^2P_{1/2}$, and $^2P_{3/2}$, the relative transition strengths for alkali-metal atoms are tabulated, e.g., in Ref. [103]. If laser light is detuned from atomic resonances, the excitation probabilities are calculated by taking into account the corresponding detunings [see, e.g., Eq. (22)]. The detunings may in turn be affected by shifts of the related energy levels, such as light shift, Zeeman shift, or the static Stark shift that can be calculated for the $^2S_{1/2}$ energy level from

$$\Delta E_{st} = -\frac{\alpha_0}{2}|\mathcal{E}_{st}|^2. \tag{26}$$

Here α_0 is the zero-frequency polarizability of the atom in this state. The light and Zeeman shifts are given by Eqs. (11) and (25), respectively. These shifts may have a significant influence on the transition probabilities, if their values are comparable with the detuning $\hbar\delta$ of the applied optical field.

3 Trapping and cooling on an evanescent-wave atom mirror

As the most important general aspects of the atom-field interaction have now been laid down, we proceed to specialized situations. In this section, we describe trapping and cooling of atoms confined above an optical evanescent wave. Among the many methods developed in the field of laser cooling and trapping, those making use of evanescent waves [96, 97, 105–109] may be of interest when creating cold atomic samples in close proximity to a solid surface. Such samples may be used for fundamental studies of low-dimensional atomic gases [109–111], investigations of near-field properties of material surfaces [112–114], and for obtaining cold atomic ensembles in surface-mounted microtraps (Publications II-V).

Typically in experiments with laser-cooled atoms, atoms are initially trapped in a standard magneto-optical trap (MOT) and then further processed depending on the specific experimental goal. Apart from some exclusions, as, for example, in guidance of atoms in hollow optical fibers [115–119], the evanescent-wave based experiments also start with this procedure. Therefore, in section 3.1, we briefly describe the main operation principles of a MOT, touching also on some aspects of cooling of atoms in optical molasses, and then proceed to the description of trapping and cooling on an evanescent-wave atom mirror (section 3.2). Finally, in section 3.3, we discuss the main factors limiting the evanescent-wave cooling efficiency, including the effect of multiple photon reabsorption, which is studied in Publication II.

3.1 Trapping in a MOT and cooling in optical molasses

Trapping of atoms in a MOT is accomplished by selective optical pumping of atoms in a spatially inhomogeneous magnetic field. The field is usually a quadrupole field produced by two identical coils carrying opposite currents. The field is therefore centrosymmetrical and such that its magnitude is equal to zero at the trap center and has approximately linear spatial dependence around it. The magnetic field results in a spatially inhomogeneous Zeeman splitting of the atomic energy levels. In addition to the magnetic field, there are three mutually perpendicular pairs of counterpropagating, circularly polarized laser beams applied on the atoms (see Fig. 3). The light frequency is chosen to match the D_2-line of the atoms and tuned to the red of a transition between two hyperfine energy levels which form a closed two-level system (see section 2.3). For ^{87}Rb, this transition is usually $|^2\mathrm{S}_{1/2}, F = 2\rangle \rightarrow |^2\mathrm{P}_{3/2}, F = 3\rangle$. According to the selection rules for the magnetic quantum number m_F, atoms in the region of both magnetic and optical fields start to scatter more light from a beam propagating towards the center of the trap than from the counterpropagating one. This results in a radiation pressure force directed

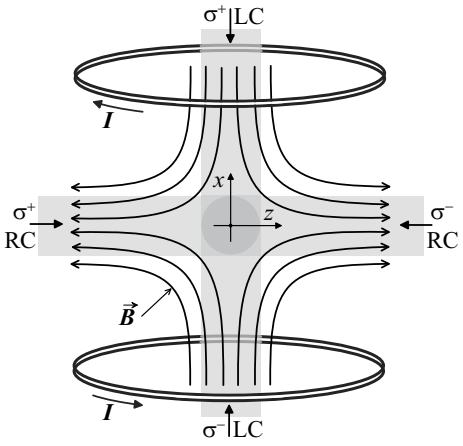

Figure 3: Schematic diagram of a magneto-optical atom trap. The laser beams are left (LC) or right (RC) circularly polarized.

towards $B = 0$. Considering atoms on a particular magnetic sublevel m_g of the ground state and taking into account the Doppler shift, $\Delta w_D = -\vec{k} \cdot \vec{v}$, the force applied to an atom from each of the counterpropagating laser beams can be written as

$$F_{\pm} = \pm\hbar k \frac{S_0\Gamma/2}{1 + S_0 + (2\delta_{\pm}/\Gamma)^2}, \tag{27}$$

where Eqs. (22) and (23) have been applied. Let us consider the two beams propagating along the z axis. If this axis is chosen to be the quantization axis, then, for atoms at positive z, the forces F_+ and F_-, as well as the detunings $\delta_{\pm} = \delta \mp \vec{k} \cdot \vec{v} \pm \mu' B/\hbar$, correspond to the σ^+- and σ^--polarized beams, respectively. Here $\mu' \equiv (g_e m_e - g_g m_g)\mu_B$. According to the selection rules, $m_e - m_g$ is equal to ± 1. The quantity μ' is always positive and, when neglecting the Doppler shift, the total force $F \equiv F_+ + F_-$ turns out to be negative. At $z < 0$, the magnetic field direction is reversed and the force is positive, so that the vector $\vec{F}$ is everywhere directed towards $z = 0$. The sign of $\vec{k} \cdot \vec{v}$ depends on the mutual directions of $\vec{k}$ and $\vec{v}$ and, without taking into account the Zeeman shift, the total force turns out to be directed against $\vec{v}$. If both the Doppler and Zeeman shifts are small compared to $\hbar\delta$, the total force can be expanded and written in the form $\vec{F} = -\beta\vec{v} - \kappa\vec{r}$, where $\vec{r}$ has its origin at $z = 0$. This force leads to a damped harmonic oscillation of the atoms around the origin. The damping rate is given by $\gamma_{MOT} = \beta/M$ and the spring constant is $\kappa = \mu'\beta A/\hbar k$, where M is the atomic mass and A the magnetic field gradient. Thus, together with trapping, a MOT provides cooling at the rate of γ_{MOT}. This cooling, called Doppler cooling, has a limit in the lowest achievable temperature, $T_D = \hbar\Gamma/2k_B$. For ^{87}Rb, for example, this limit is $T_D = 146$ μK.

In practice, the temperature can drop even bellow the Doppler limit, since the light field of the MOT has polarization gradients, which leads to an additional, so-called polarization gradient cooling of the atoms.

Along with the cycling transitions $F_g \leftrightarrow F_e$ between two selected hyperfine states, there is a small probability for the atoms to be excited into the neighboring hyperfine state with $F_e = F_g$. Such atoms can then undergo spontaneous emission to another hyperfine ground state, F_g', and, as a result, escape from the trap. In order to prevent this loss, the atoms from the state F_g' are continuously pumped back to the state F_g, using a laser beam tuned into resonance with, e.g., a D_1 transition between F_g' and a certain F_e state.

A usual procedure to further decrease the temperature is to switch the magnetic field off and lower the intensity of the MOT beams together with increasing the detuning. This leads to polarization gradient cooling in the σ^+-σ^- optical molasses. To qualitatively explain the cooling scheme, it is sufficient to consider only two counterpropagating beams. Their total field has a spatially rotating linear polarization. The quantization axis for the atoms rotates together with the direction of the field polarization and, in order to follow it, moving atoms should experience optical transitions. For atoms moving toward the σ^+-polarized beam, the transitions tend to populate the magnetic substates with $\Delta m_g = +1$, which leads to a substantial increase of the scattering rate from this beam due to an increased transition strength. Similar situation takes place for atoms moving in the opposite direction. The atomic motion is therefore damped towards $v = 0$. The final temperature can be an order of magnitude lower than the Doppler limit and only several times higher than the recoil limit $T_r = (\hbar k)^2/Mk_B$.

3.2 Trapping and cooling on an evanescent-wave mirror

A theoretical model describing cooling of atoms on a tilted evanescent-wave mirror was introduced by J. Söding *et al.* in [105], and it has since been applied to calculate the cooling parameters in a variety of trap configurations [105, 120–124]. Experimentally, the cooling was demonstrated using a gravito-optical surface trap [105, 120, 121], which was constructed for the purpose of achieving quantum degeneracy of ^{133}Cs [99, 108, 109]. A gravito-optical surface trap (GOST) is formed by a horizontally aligned EW mirror, the action of gravity, and a blue-detuned hollow laser beam (see Fig. 4a). A hollow beam can be obtained from a Gaussian beam, e.g., by modifying it with an optical system containing an axicon [98, 125, 126]. In Publication I, we introduce an alternative technique, where a similar modification is provided by using self-phase modulation of a Gaussian laser beam in a nematic liquid crystal. Thin-walled hollow beams of different sizes and peak intensities have been created using a very simple and cheap optical system (see Fig. 5), which is characterized by a high power conversion efficiency, insensitivity to alignment of

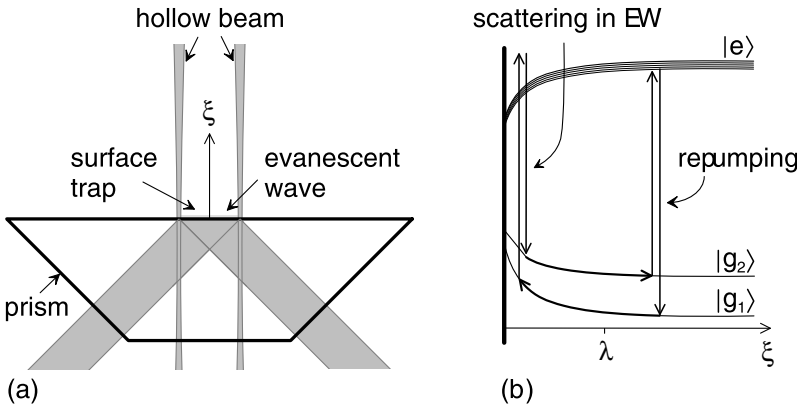

Figure 4: (a) Gravito-optical surface trap. (b) Cooling transitions between EW-shifted energy levels of the atoms.

the optical elements, and the ability to produce non-diverging, as well as converging or diverging beams.

Loading of atoms into a GOST is performed in several steps. First, atoms are trapped and cooled in a MOT located a few millimeters above the GOST. Then, the MOT is switched off and the atoms are allowed to fall inside the hollow beam towards the evanescent-wave mirror. Under gravity, the atoms make inelastic reflections off the evanescent wave, which leads to an efficient cooling of the sample. The process is completed, when the temperature has reached an equilibrium and the EW frequency further detuned from the atomic resonance in order to increase the trap lifetime.

The basic equations describing the cooling process can be derived by considering a single atom which, nevertheless, exchanges its kinetic energy with the other atoms in the trap. All relevant quantities are described in terms of their mean values per atom. The intensity of the evanescent wave created by total internal reflection decays exponentially above the surface with a decay length of $\Lambda = (\lambda/4\pi)(n^2 \sin^2\theta - 1)^{-1/2}$. Here λ is the laser wavelength, n the index of refraction of the dielectric, and θ the angle of incidence of the reflected beam. As in Ref. [105], we assume the evanescent wave to be a monochromatic and linearly polarized wave tuned above the D_2-resonance frequency by an amount δ which is much larger than the hyperfine splitting of the excited state, $|e\rangle$. The detuning is measured with respect to the lower hyperfine ground state. Under the approximation of small saturation, the optical potentials (the light shifts) can be written as $U_1(\xi) = (2/3)\hbar\Omega^2(\xi)/4\delta$ and $U_2(\xi) = (2/3)\hbar\Omega^2(\xi)/4(\delta + \delta_{hfs})$ for the lower, $|g_1\rangle$, and upper, $|g_2\rangle$, hyperfine ground states, respectively. Here δ_{hfs} is the ground-state hyperfine splitting and $\Omega(\xi) = \Gamma\sqrt{I(\xi)/2I_{sat}}$ is the Rabi frequency discussed in

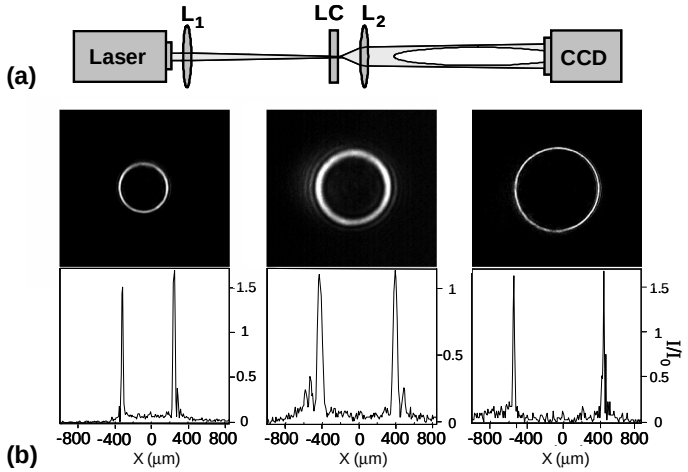

Figure 5: (a) Experimental setup for creation of a hollow laser beam using a nematic liquid crystal (LC) and two lenses (L_1 and L_2). (b) CCD images of three different hollow beams together with intensity profiles along a line crossing the beam axis (I_0 is the peak intensity of the incident Gaussian beam in the CCD plane).

section 2. Compared to Eq. (12), the potentials U_1 and U_2 include an extra factor of 2/3, which stems from the sum of the transition strengths over the excited-state hyperfine levels [105]. Note that the potential U_2 can be considerably smaller than U_1 because of the larger detuning, $\delta + \delta_{hfs}$. The atomic energy levels shifted by the EW field are schematically shown in Fig. 4b.

In the presence of a downward propagating, low-power repumping beam the atoms are slowed down. The repumper is tuned into resonance with the transition $|g_2\rangle \rightarrow |e\rangle$ in order to optically pump atoms that have entered $|g_2\rangle$ back into the state $|g_1\rangle$. If an atom in the state $|g_1\rangle$ enters the repulsive evanescent wave and, near the turning point, makes a transition to the state $|g_2\rangle$ (through scattering of an evanescent-wave photon), the energy lost by the atom as it climbs up the potential hill will be larger than that it gains when leaving the field after the reflection. Recycling the process leads to a *Sisyphus* cooling of the atoms at the rate [105]

$$\gamma_{Sis} \approx \frac{2}{9} \frac{\delta_{hfs}}{\delta + \delta_{hfs}} \frac{1 - q_e}{\tau_c}, \tag{28}$$

where q_e is the mean branching ratio to the lower hyperfine ground state for elastic scattering of a photon. The parameter τ_c denotes the mean time between incoherent reflections, which is given by

$$\tau_c = \frac{\hbar \delta}{\Gamma \Lambda M g \sin \varphi}, \tag{29}$$

where M is the atomic mass, g the acceleration due to gravity, and φ the angle between the vertical axis and the vacuum-dielectric interface.

The rate of the *geometric* cooling, originating from the absorption of the downwards propagating repumping photons by the $|g_2\rangle$-state atoms on their way up in the gravitational field, is calculated to be

$$\gamma_{geo} \approx \frac{4\pi\hbar \sin\varphi}{3\lambda q_r \sqrt{M k_B T}} \frac{1-q_e}{\tau_c}, \tag{30}$$

where q_r is the mean branching ratio to the state $|g_1\rangle$ for transitions in the repumping field starting from the state $|g_2\rangle$, k_B is the Boltzmann's constant, and T the instantaneous temperature of the atoms. Since τ_c is inversely proportional to $\sin\varphi$, the rate γ_{geo} is proportional to $\sin^2\varphi$.

Assuming that in each optical transition the kinetic energy of an atom increases by one photon recoil energy, one can find the expression for the corresponding heating rate (see Ref. [105]) to be

$$\gamma_{heat} = \left(2 + \frac{1-q_e}{q_r}\right) \frac{(2\pi\hbar)^2}{3\lambda^2 M k_B T} \frac{1}{\tau_c}. \tag{31}$$

In thermal equilibrium, the heating rate is equal to the overall cooling rate,

$$\gamma_{heat} = \gamma_{Sis} + \gamma_{geo}, \tag{32}$$

and the solution of this equation with respect to T gives the final temperature T_{eq}. In the case of perfect alignment, φ is equal to $\pi/2$ and

$$T_{eq} = C_1^2 \left(\sqrt{1 + C_2 \left(\frac{2q_r}{1-q_e} + 1 \right)} - 1 \right)^2, \text{ where} \tag{33}$$

$$C_1 \equiv \frac{3(\delta + \delta_{hfs})\pi\hbar}{\delta_{hfs} q_r \lambda \sqrt{M k_B}} \text{ and} \tag{34}$$

$$C_2 \equiv \frac{2q_r \delta_{hfs}}{3(\delta + \delta_{hfs})}. \tag{35}$$

In deriving this equation, we assumed that $(1-q_e)2\pi\Lambda\Gamma/q_r\lambda\delta \ll 1$. The equilibrium temperature for ^{87}Rb ($\delta_{hfs} \approx 2\pi \times 6.8$ GHz, $q_e \approx 0.72$ and $q_r \approx 0.62$ [105]) when $\delta = 2\pi \times 1$ GHz is $T_{eq} = 1.4$ μK which is only 4 times higher than the recoil limit $T_r = 0.36$ μK. For ^{133}Cs ($\delta_{hfs} \approx 2\pi \times 9.2$ GHz, $q_e \approx 0.75$ and $q_r \approx 0.61$ [105]), we obtain $T_{eq} = 0.9$ μK, while $T_r = 0.20$ μK. The equilibrium temperature is reached in a time comparable to $1/\gamma_{Sis}$ which, at relevant parameter values, is on the order of 1 s [105]. We remind the reader that the present model implies instantaneous thermalization of the sample at each moment of the cooling process. The realistic cooling time depends also on the atom density and the trap size, and usually it extends to several seconds [120].

3.3 Evanescent-wave cooling limits

According to the model described in the above section, the temperature of the evanescent-wave cooled atoms can decrease down to a value of about $4T_r$. The lowest temperature which has been achieved so far in the experiments with *low-density* atomic samples of ^{133}Cs is two times higher than this calculated value [121]. One of the possible reasons can be a "roughness" of the realistic evanescent-wave mirror which leads to a diffuse atomic reflection [113] and, as a result, to a decrease of the geometric-cooling efficiency (see $\sin\varphi$ in Eq. (30)). Other effects, such as scattering of light at imperfections on the prism's surface and possible optical transitions in the field of the hollow beam, may also take place. Besides these essentially technical reasons, multiple reabsorption of resonance-frequency photons in the cooled sample can have a noticeable influence on the temperature. In Publication II, we have taken into account this effect and derived the dependence of the minimum achievable temperature on the number of atoms in the sample and on the effective size of the trap. The approach is based on the law of energy conservation. We start by calculating the mean rate per atom, R_{in}, at which the resonant photons originally appear in the sample due to the transitions $|e\rangle \rightarrow |g_1\rangle$ completing each cooling cycle. The total power of these photons, $P_{in} = 2\pi\hbar\nu_1 R_{in}$, is equal to the power P_{out} of the resonant photons escaping from the sample, which gives a mean rate of $R_r = (1/\eta_{out} - 1)R_{in}$ for the reabsorption of photons by each atom. The rate R_{in} is given by $R_{in} \approx (1 - q_e)/2\tau_c$. The parameter η_{out} defines the ratio of the escaping power P_{out} per atom to the overall resonance-frequency power $P_{rad} \equiv 2\pi\hbar\nu_1(R_{in} + R_r)$ emitted on average by each atom. Assuming that each transition is associated with an increase of the atomic kinetic energy by one recoil energy, we derive an expression for the heating rate $\widetilde{\gamma}_{heat}$ which includes the influence of the multiple reabsorption of photons as

$$\widetilde{\gamma}_{heat} \approx \left(2 + \frac{1 - q_e}{q_r \eta_{out}}\right) \frac{(2\pi\hbar)^2}{3\lambda^2 M k_B T} \frac{1}{\tau_c}. \tag{36}$$

Compared with Eq. (31), this equation contains the parameter η_{out}. Since η_{out} is always smaller than 1, the rate $\widetilde{\gamma}_{heat}$ is always higher than γ_{heat}, and only if the resonance-photon reabsorption can be neglected is $\eta_{out} \approx 1$ and $\widetilde{\gamma}_{heat} \approx \gamma_{heat}$. Equating now $\widetilde{\gamma}_{heat}$ to $\gamma_{Sis} + \gamma_{geo}$, we find the corrected equilibrium temperature $\widetilde{T}_{eq}$ to be given by

$$\widetilde{T}_{eq} = C_1^2 \left(\sqrt{1 + C_2 \left(\frac{2q_r}{1 - q_e} + \frac{1}{\eta_{out}}\right)} - 1\right)^2, \tag{37}$$

with C_1 and C_2 given by Eqs. (34) and (35). To calculate the parameter $\eta_{out} \equiv P_{out}/P_{rad}$, one may assume that the atomic sample has a constant density equal

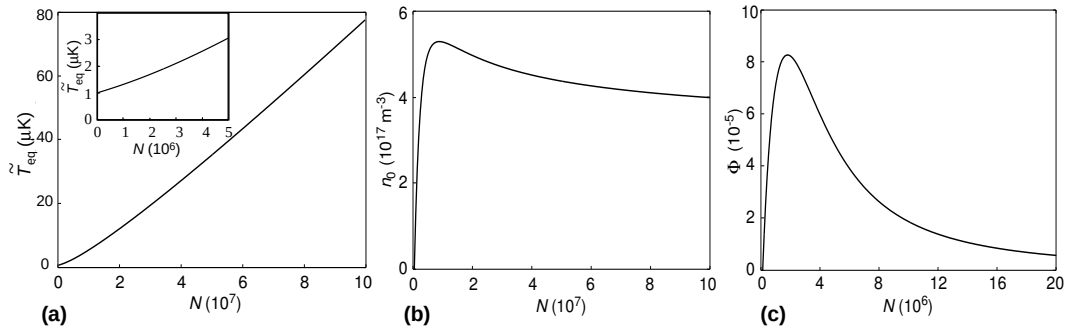

Figure 6: Dependence of (a) equilibrium temperature, (b) number density, and (c) phase-space density of ^{133}Cs in a GOST on the total number of atoms N. [Publication II]

to the peak density n_0 within the effective volume of the trap. Then, by modelling the emitted resonance-frequency photons as attenuating spherical waves radiated by each atom at power P_{rad}, one can obtain an estimate for the power P_{out} and thus find η_{out}. The attenuation coefficient for weak resonance-frequency radiation in the case of a lifetime-broadened transition may be taken in the form $\alpha \approx 3n_0\lambda^2/2\pi$ [103].

For a GOST with a diameter D being much larger than the thermal height $u \equiv k_BT/Mg$ of the sample, the parameter η_{out} takes the form

$$\eta_{out} = \frac{1 - e^{-\zeta}}{2\zeta} - \frac{1}{2}[\zeta\Gamma(0,\zeta) - \mathrm{e}^{-\zeta}], \tag{38}$$

where $\Gamma(0,\zeta)$ is the incomplete gamma function and $\zeta \equiv \alpha u$ is equal to $6N\lambda^2/(\pi D)^2$. Here N is the total number of atoms in the trap. The attenuation coefficient α is proportional to the density $n_0 = N/(u\pi D^2/4)$ and, therefore, ζ is independent of u. Substituting Eq. (38) into Eq. (37), we can calculate the equilibrium temperature $\widetilde{T}_{eq}$.

As an example, we show the calculated dependencies of the temperature $\widetilde{T}_{eq}$ (Fig. 6a), peak number density n_0 (Fig. 6b), and phase-space density Φ (Fig. 6c) on the number of atoms N for ^{133}Cs atoms cooled in a GOST. The values for the hollow beam diameter, $D = 0.8$ mm, and the evanescent-wave detuning, $\delta = 2\pi \times 5$ GHz, have been taken from Refs. [108] and [109]. The phase-space density is given by $\Phi = (n_0/7)(2\pi\hbar^2/Mk_B\widetilde{T}_{eq})^{3/2}$. The resonance-photon reabsorption is seen to significantly affect the final temperature of the cooled atoms. The lowest possible temperature in cooling of, e.g., 10^8 atoms is almost two orders of magnitude higher than T_{eq} calculated from Eq. (33). Both the number density n_0 and the phase-space density Φ versus the number of atoms show a well established maximum. The phase-space density reaches its maximum value of $\Phi_p \approx 8 \times 10^{-5}$ at $N \approx 2 \times 10^6$.

This value can in principle be increased by reducing the trap size, since the trapped resonant radiation escapes smaller samples more efficiently (see Publication II). On the other hand, if the number of atoms to be trapped is fixed, the trap cannot be reduced to an arbitrarily small size, since at higher densities the trap lifetime becomes shorter due to inelastic interatomic collisions. In this case, the cooling efficiency could be improved, if the repumping mechanism was replaced with a process that would not involve spontaneously emitted resonance-frequency photons. Such repumping could be realized through Raman transitions in a field which does not contain near-resonance frequency components.

4 Microscopic atom traps on an evanescent-wave mirror

The idea of creating surface-mounted atom traps and guides emerged at the end of the 1990s on the basis of experiments on the manipulation of atoms with free-standing charged and current-carrying wires [101, 127–131]. It was then realized that making the wires narrower could bring about several important advantages. Already in 1996 Vuletic *et al*. demonstrated a miniaturized magnetic quadrupole trap allowing one to increase both the atom density and trap level spacing in order to provide more efficient evaporative cooling [132]. To create a comparable steep and tight potential with a thick free-standing wire, current (or voltage) has to be impractically high. Thus, the wire thickness should be substantially reduced, to, say, ~ 10 μm. In current-based experiments, however, such a thin wire would be difficult to exploit due to, e.g., mechanical instability which can be caused by thermal expansion induced by the current. If, on the other hand, the wire is lithographically fabricated on a solid substrate, the trap is stable and has a well-defined position. In addition, higher current densities can be used, because the substrate serves as a heat dissipator. J. Schmiedmayer in his pioneering paper on this subject [100] has listed the main advantages of the microscopic atom traps on a solid substrate to be (a) simplification of storage of atoms in the trap ground state and creation of single-mode atom waveguides, (b) the possibility to integrate many atom-optical components into a single device, "atom chip", and (c) the possibility to realize coupling between the states of atoms in different trapping sites, which can be used, e.g., in quantum information processing.

The problem of loading a small surface-mounted trap with atoms was solved by the invention of the *mirror* MOT [68, 133]. The mirror MOT can provide trapping and cooling of atoms at a distance of a few millimeters above the surface which is coated with a thin metal film in order to reflect two of the MOT's beams. In most of the current experiments, the microtraps are based on current-carrying wires, and the loading procedure typically includes such stages as (1) transfer of atoms from a mirror MOT into a so-called U-MOT (created with a thick U-shaped wire on or below the substrate), (2) cooling using optical molasses, (3) replacement of the U-MOT with a spatially matched purely magnetic trap, and (4) transfer of the atoms to smaller and steeper traps or guides formed by thin conductors. A similar loading technique has been used to demonstrate the feasibility of surface-mounted traps in the creation of a Bose-Einstein condensate [66, 134]. It has also been demonstrated that an atomic sample can be loaded into a surface-mounted trap by transporting the sample in a macroscopic magnetic [135] or red-detuned optical [136] trap.

In regard to the creation of BEC, phase-space density is the key parameter. When using a microtrap, the phase-space density is increased to the level of quantum degeneracy in a traditional way by applying rf-forced evaporative cooling. Be-

fore starting the evaporation, the phase-space density in the microtrap is typically lower than 10^{-5}. However, because of a high number density of the atoms, typically $n_0 > 10^{10}$ cm^{-3}, and a small size of the trap, the evaporative cooling can be made to proceed quickly. The trapping frequencies are usually not very high, on the order of 1 kHz, which is in particular dictated by the necessity to position the trap center at a large distance from the metal coating of the substrate (typically $> 10\ \mu$m). This is explained by the influence of the thermal motion of free electrons in the metal on the coherence time of the trapped atomic sample [66, 83, 84]. The magnetic field fluctuations near the surface cause transitions of the atoms to other magnetic states, which also leads to reduction of the trap lifetime. Similar magnetic-field fluctuations are caused by the technical noise of currents in the wires. Since these fluctuations scale with the strength of the trapping potential, they can not be reduced simply by increasing the trap-surface separation and, therefore, a careful stabilization of the current source is of particular importance.

One of the goals of the research work described in this thesis is to develop a method for creation of surface-mounted microtraps and guides which would not require metal coating of the substrate, but which still could be efficiently loaded with atoms. We also consider a trapping technique which does not involve currents, but, instead, allows easy access to the trapped atoms with light. This can be achieved in practice if the substrate is made of light-transparent material. A number of promising experimental results on trapping and cooling of atoms in a gravito-optical surface trap [96, 97, 99, 108, 109] have supported our idea to develop microtraps based on an evanescent-wave mirror. In section 4.1 we describe the basics of creation of such microtraps, and in section 4.2, we analyze the loading of them with atoms from a GOST. Section 4.3 presents a generalized theoretical model for describing a multicomponent atom sample in a trap containing a tight and deep subtrap.

4.1 Trap designs

A microscopic electro-optical atom trap on an evanescent-wave mirror

The possibility to create a surface-mounted atom trap on an evanescent-wave atom mirror was first mentioned by J. Schmiedmayer in the discussion of trap designs based on an electrically charged wire [100]. Realization of such an electro-optical trap, where an optical potential prevents atoms from attaching to the wire, is of interest, since it allows storing atoms independently of their magnetic states. Moreover, the collisional properties of atoms in such traps can be magnetically tuned using Feshbach resonances without influence on the shape of the trapping potential. To electrically charge the wire, one must place it close to another conductor and connect them to different electric potentials. The charge density and, consequently, the resulting electric field strength will depend on the applied voltage and on the

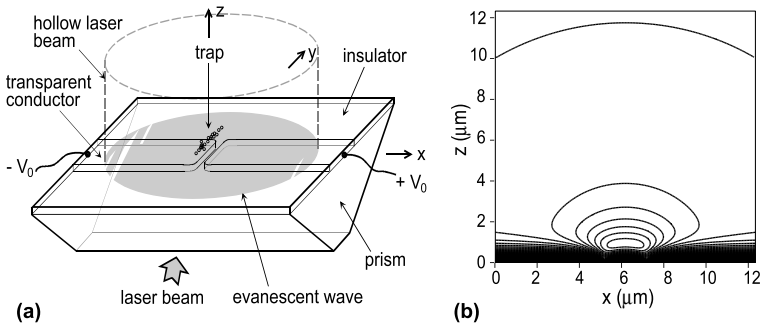

Figure 7: (a) Schematic diagram for realizing an electro-optical atom trap on an EW atom mirror. (b) Equipotential contours of the interaction potential. The step size between the contour lines is ~ 2 μK. [Publication III]

distance between the wire and the conductor. Instead of using a wire, our design for an electro-optical atom trap is based on the use of two oppositely charged transparent electrodes (made of, e.g., indium tin oxide) separated by a distance of a few μm [Publication III]. The electrodes are embedded in a refractive-index-matched thin dielectric film on the surface of a glass prism, as is schematically shown in Fig. 7a. We also indicate in the figure how the trap can be combined with a gravito-optical surface trap. A suitable material for the dielectric layer could be noncrystalline silicon nitride [137]. The design allows for (1) a strong electric field to be created above the gap between the electrodes using a low-voltage source and (2) a smooth evanescent-wave mirror for the atoms to be created on the film surface by total internal reflection of a blue-detuned laser beam, as a result of which an efficient cooling of atoms on the evanescent wave can be conducted before loading the trap.

The potential of interaction between an atom and the static electric field and the evanescent wave is given by

$$U = -\frac{\alpha_0}{2k_B}|\mathcal{E}_{st}|^2 + \frac{\lambda^3}{8\pi^2 c k_B}\frac{\Gamma}{\delta} I_0 \exp(-z/\Lambda), \tag{39}$$

where U is expressed in units of temperature. The first term in this expression introduces the static Stark shift [see Eq. (26)] and the second term is the light shift (see page 15). The parameter α_0 denotes the electric polarizability of the atom, I_0 the maximum value of the evanescent-wave intensity, z the height above the film surface, and Λ the intensity decay length of the evanescent wave. Equation (39) has been written for an atom in the lower hyperfine ground state in the limit of low saturation in the evanescent wave. Both gravity and the van der Waals interaction have been neglected [105, 138, 139]. For ^{133}Cs, for example, the energy "shift" due to gravity is less than 1 μK at $z = 10$ μm. Also, the evanescent-wave intensity is

chosen to prevent van der Waals attraction so that the potential barrier between the potential minimum and the surface remains much higher than the expected thermal energy of the atoms. As an explicit example, we show calculated equipotential contours for atoms of ^{133}Cs ($\alpha_0 = 6.6 \times 10^{-35}$ C·cm^2/V) above a 2 μm gap between 100 nm thick electrodes with a voltage drop of 0.62 V across them (see Fig. 7b). The peak intensity I_0 is chosen to be 1×10^8 W/m^2 corresponding to total internal reflection of a p-polarized laser beam of 2.5 W with a beam diameter of 0.6 mm (the incident angle is 31°; the decay length is $\Lambda \approx 0.32\lambda$). The laser wavelength is detuned from the D_2-resonance by -15 nm. This atom trap is 13.6 μK deep and has transverse dimensions on the order of a micrometer. The longitudinal size of the trap (in the y direction) is determined by the y size of the electrodes.

Owing to the large detuning of the evanescent wave from the atomic resonance, the mean time between successive optical transitions of an atom located at the minimum of the confining potential is long, approximately 2 seconds [Publication III]. Within this time, the optical transitions can cause heating of the trapped atoms by $\Delta T \approx 2E_r/3k_B$, where E_r is the recoil energy. Note that the factor of 1/3 in this expression comes from the equipartition theorem. The value of ΔT is 66 nK and the corresponding heating rate is 33 nK/s. Along with this essentially slow heating of the sample, the optical transitions will also cause a loss of atoms from the trap. The loss rate caused by two-body collisions between atoms in different quantum states is proportional to the number density n of the atoms, while the rate due to three-body recombination is proportional to n^2. At high densities, the main loss mechanism for ^{133}Cs will be due to three-body recombinations.

A microscopic magneto-optical atom trap on an evanescent-wave mirror

A microscopic magnetic trap that can be combined with an evanescent-wave mirror can be created either by a current-carrying conductive or permanently magnetized structure made of optically transparent material. As in the previous example, the conductive material may be indium tin oxide. A promising material for the magnetic structure is a ferrimagnetic bismuth- and gallium-substituted iron garnet, which is well transparent to light at $\lambda > 600$ nm and has high coercivity and remnant magnetization. Owing to these properties, a thin film of this material can be uniformly magnetized and then the magnetization direction can be locally reversed, resulting in the creation of a strong magnetic field above the magnetization-flipped pattern. Even patterns with sub-micrometer widths are possible to realize with conventional magnetic recording methods. We have examined the possibility to selectively magnetize such a thin iron-garnet film by exposing it locally to a focused laser beam ($\lambda = 532$ nm) and applying a bias magnetic field from a macroscopic permanent magnet. We have succeeded in magnetizing narrow strips and dots with a characteristic size of < 5 μm in a 3 μm thick iron-garnet layer. Selectively magnetized

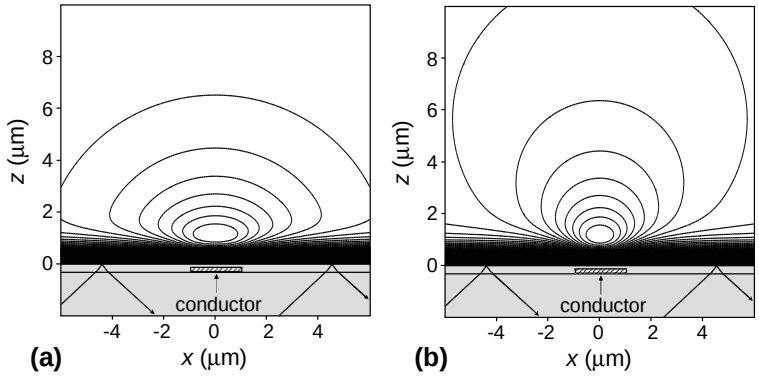

Figure 8: Equipotential contours of the trapping potential U with a step of 2 μK above a current-carrying transparent wire for ^{87}Rb in (a) high-field seeking $|5^2\mathrm{S}_{1/2}, \mathrm{F} = 1, \mathrm{m_F} = +1\rangle$ state, and (b) low-field seeking state $|5^2\mathrm{S}_{1/2}, \mathrm{F} = 1, \mathrm{m_F} = -1\rangle$. The trap for low-field seeking atoms is obtained by applying a bias magnetic field along the x axis. [Publication IV].

films are essentially homogeneous for light, since the refractive index of the material does not depend on the magnetization direction. Conductive structures, on the other hand, should be imbedded in a dielectric layer with equal index of refraction.

In the following we describe a microtrap, where the magnetic potential is created by a transparent conductor, although a permanently magnetized structure can be used as well. As with the electro-optical trap in the previous example, the magneto-optical trap can be created inside a gravito-optical surface trap. The experimental setup in this case may be similar to the one shown in Fig. 7a, but instead of the electrodes, the film will contain a current-carrying wire [Publication IV]. Let the wire be in the simple form of a straight conductive strip. The potential of interaction of an alkali atom with a static magnetic field, no matter which way it is produced, and the evanescent wave reads

$$U = \frac{1}{k_B} g_F m_F \mu_B |\mathbf{B}| + \frac{\lambda^3}{8\pi^2 c k_B} \frac{\Gamma}{\delta} I_0 \exp(-z/\Lambda), \tag{40}$$

where, as in Eq. (39), U is expressed in units of temperature. The first term in Eq. (40) introduces the Zeeman shift given by Eq. (25). The parameter g_F stands for the Landé g-factor, μ_B for the Bohr magneton, $\mathbf{B}$ for the magnetic-field induction, and m_F for the projection of the total angular momentum $\mathbf{F}$ on the magnetic-field direction. The evanescent-wave detuning δ is assumed to be much larger than the Zeeman splitting of the magnetic energy levels. Figure 8a shows the equipotential contours of U with a step of 2 μK for ^{87}Rb in the state $|F = 1, m_F = +1\rangle$ of the ground state $5^2\mathrm{S}_{1/2}$ (the high-field seeking atoms) above a current-carrying strip

located 100 nm below the surface and having a thickness of 200 nm and a width of 2 μm. The strip carries a current of 0.43 mA. The intensity I_0 is equal to 6×10^7 W/m^2. The detuning δ and the decay length Λ are 4500 GHz ($\Delta\lambda = -9$ nm) and 250 nm, respectively. The trap is 18 μK deep and has transverse dimensions on the order of a micron. The distance of the potential minimum from the surface is approximately 1 μm. The longitudinal size of the trap may be limited, e.g., by making the strip much wider outside the trapping region.

The trap of Fig. 8b for ^{87}Rb in the state $|F = 1, m_F = -1\rangle$ (low-field seeking atoms) is obtained by applying a bias magnetic field of $\widetilde{B} = 5$ G solely along the x axis. For this trap, the point where the total magnetic field has zero strength is located below the film surface and, therefore, no Majorana spin flips can occur. The trap has approximately the same depth and position above the film as the trap of Fig. 8a. However, the trapping frequency in the horizontal direction near the bottom is higher, $\sim$ 40 kHz compared to $\sim$ 20 kHz in the high-field seeker trap. The frequency in the vertical direction is approximately the same in both traps, and roughly equal to 60 kHz.

The atoms in both microtraps considered are localized in a region of non-zero light intensity. However, the mean time between optical excitations of the atoms in the trap is as long as 2 s. The optical transitions will nevertheless cause some loss of atoms from the microtrap due to (1) optical transitions to the untrapped magnetic substates of the lower hyperfine ground state $|F = 1\rangle$ and (2) transitions to the trapped substates which belong to the upper hyperfine ground state $|F = 2\rangle$ (the atoms in these states will participate in binary hyperfine-state exchange collisions, which, in the case of high atomic density, will lead to a fast loss of the participants [140]). At high densities, the loss rate due to the optical transitions will be on the order of 0.5 s^{-1}. The three-body-recombination loss rate $\gamma_{3b} = L_{3b}n^2$ is rather low for ^{87}Rb due to the smallness of the coefficient L_{3b}, which is on the order of 4×10^{-30} cm^6/s [141].

4.2 Loading technique based on local phase-space compression

The phase-space density of a trapped atomic sample can be significantly increased by deforming the trapping potential [26,99,108,142–144]. Particularly high density values can be achieved by adding a tight and deep potential to a wide trap [26, 99, 108]. In this case, the peak number density, dictated by the *depth* of the new trap, can exceed the initial density by several orders of magnitude. By making the *volume* of the new trap much smaller than the volume of the original trap, one can ensure the temperature to remain low. This results in a strong local increase of the phase-space density [26, 99, 108]. The loading technique described in this section is based on this effect.

Loading of a surface-mounted electro-optical trap

For an electro-optical atom trap on an EW mirror (see section 4.1), the loading procedure may be similar to the one described in Ref. [108]. Let such a trap suddenly appear within a GOST containing already a cold atomic sample. Both the electric and optical potentials are independent of atom spins. As a result, the subtrap will be equally populated by atoms in different magnetic states. If the sample is completely unpolarized, the phase-space density will be a factor of 3 lower for ^{87}Rb and a factor of 7 for ^{133}Cs than it would be if the sample was spin-polarized. For a moment, we will ignore this factor and assume that the atoms are all in a single magnetic state.

Being dependent on the number of atoms transferred into the subtrap, the increase of the atomic temperature in the loading process can be small. Denoting the total number of the atoms by N_t, their initial temperature by T_i, the effective GOST volume by V_{GOST}, and the subtrap volume by V_{st}, we can assess the number of atoms transferred into the subtrap, N_{st}, and the final temperature, T_f, by solving the coupled equations

$$T_f = T_i + \frac{2}{3}\Delta U_{st}\left(\frac{N_{st}}{N_t} - \frac{V_{st}}{V_{GOST}}\right), \tag{41}$$

$$\frac{N_t - N_{st}}{V_{GOST} - V_{st}} = \frac{N_{st}}{V_{st}}\exp\left(-\frac{\Delta U_{st}}{T_f}\right), \tag{42}$$

where ΔU_{st} is the subtrap depth in units of temperature. The above equations are obtained by requiring conservation of energy and assuming a Maxwell-Boltzmann density distribution for the atoms. For simplicity, both the GOST and the subtrap potentials are assumed to be square-wells. Let the GOST initially contain 2×10^6 atoms of ^{133}Cs (the number is as in Ref. [108]) at a temperature T_i of 2 μK (two times higher than the theoretical one calculated in section 3.2). If the volume V_{GOST} is equal to 6.4×10^{-12} m^3, corresponding to a GOST diameter of 0.8 mm, and the subtrap volume is $V_{st} = 5 \times 10^{-16}$ m^3 (the width of the electrodes is ~ 100 μm), then, in the case of $\Delta U_{st} = 13.6$ μK, the number of atoms in the subtrap is calculated to be $N_{st} \approx 6 \times 10^4$ and the temperature to be $T_f \approx 2.3$ μK. The local density of atoms in the microtrap is $n_0 \approx 1 \times 10^{20}$ m^{-3} and the local phase-space density $\Phi_{st} \equiv n_0\left(\hbar\sqrt{2\pi/Mk_BT}\right)^3 \approx 0.1$. If no efforts are made to spin-polarize the sample before inserting the subtrap, the phase-space density will be 7 times lower. Nevertheless, such a high phase-space density is difficult, if not impossible, to reach in conventional microtraps on current-carrying wires [66, 68, 135, 145] without applying additional cooling by evaporation. Note that the loading technique in the latter case would transfer the whole atomic ensemble into the microtrap and, consequently, no similar gain in the phase-space density could take place in the loading process. We finally note that for efficient loading of a microtrap from a GOST, the

thermalization rate of atoms in the GOST has to be higher than the loss rate of atoms from the microtrap. In the case considered here, this condition is well satisfied.

Loading of a surface-mounted magneto-optical trap

Let now a magnetic subtrap suddenly appear within the GOST containing a spin-unpolarized sample of ^{87}Rb. We assume the total number of atoms to be the same as in the previous example, $N_t = 2 \times 10^6$, and the temperature to be about two times higher than that calculated in section 3.2, i.e., $T_i = 3$ μK. The effective volume of the GOST is now $V_{GOST} = \pi(400\ \mu\text{m})^2 \times 30\ \mu\text{m}$, where 400 μm is the GOST radius and 30 μm is the thermal height of the atomic sample above the evanescent-wave mirror. For the sake of generality, we denote the magnetic quantum states of the atoms in the lower hyperfine ground state by $|m_a\rangle$, $|m_F = 0\rangle$, and $|m_r\rangle$, where the subindices a and r denote states which are attracted and repelled by the subtrap, respectively. Thus, independently of the kind of subtrap, the trapped state is $|m_a\rangle$. The subtrap depth for this state is assumed to be $\Delta U_{st} = 18$ μK. After the appearance of the subtrap, the final number N_a and temperature T_f of atoms in the subtrap can be calculated by solving the following coupled equations

$$T_f = \frac{1}{3}(T_a + T_0 + T_r), \text{ where } T_0 = T_r = T_i, \tag{43}$$

$$T_a = T_i + \frac{2}{3}\Delta U_{st}\left(\frac{N_a}{N_t/3} - \frac{V_{st}}{V_{GOST}}\right), \tag{44}$$

$$\frac{N_t/3 - N_a}{V_{GOST} - V_{st}} = \frac{N_a}{V_{st}} \exp\left(-\frac{\Delta U_{st}}{T_f}\right). \tag{45}$$

Similarly to Eqs. (41) and (42), the above equations are obtained by applying the law of energy conservation. The Maxwell-Boltzmann density distribution for the atoms is applied separately to each of the magnetic states. We have also taken into account the fact that the magnetic field forming the subtrap has no influence on the atoms in the state $|m_F = 0\rangle$ and only a minor influence on the repelled-state atoms. The auxiliary variables T_0 and T_r, which are the temperatures that could be reached by the sample if the atoms were initially spin-polarized into the $|m_F = 0\rangle$ or $|m_r\rangle$ state, respectively, are therefore equated to T_i. In the GOST, the volume V_{st} of the subtrap has an upper limit of about 5×10^3 μm^3 corresponding to the case when the subtrap length is equal to the GOST diameter. In this case, the number of atoms transferred into the microtrap is $N_a = 5 \times 10^4$, the final temperature is $T_f = 3.3$ μK, the peak number density is $n_0 = 1 \times 10^{19}$ m^{-3}, and the phase-space density is $\Phi_{st} \approx 0.01$. This value is on the same order of magnitude as the one calculated for spin-unpolarized atoms of ^{133}Cs in the previous example. However, while initial spin-polarizing of cesium would result in several times higher phase-space density, it will not significantly influence the phase-space

density in the present example, since the latter is already at the same high level as it would be had the sample initially been spin-polarized. The Zeeman splitting of the atomic energy level, ΔE_Z, by far exceeds the thermal energy of the atoms. In the high-field seeker trap of Fig. 8a, it is $\Delta E_Z = 20$ μK, and in the trap of Fig. 8b, ~ 100 μK. At a temperature of a few μK, essentially all atoms in the subtrap are in a single magnetic state $|m_a\rangle$. The rest of the atoms are still stored in the GOST, contributing to the peak phase-space density through keeping the temperature from increasing. Thus, when using this method, there is no need for spin polarization.

After the loading is completed, the "thermostat" atoms can be released from the GOST and the sample in the microtrap can be further processed. A high value of the phase-space density on the trap bottom enables providing favorable conditions for efficient evaporative cooling and achievement of Bose-Einstein condensation.

4.3 Thermodynamics of a multicomponent atom sample in a locally compressed atom trap

In this section we describe in general terms the response of a trapped multi-species atomic sample to a local deformation in the confining potential (Publication V). In contrast to a deformation caused by abruptly switching on a subtrap in section 4.2, the deformations in this section are considered to be inserted or removed adiabatically. Using the model, which is based on classical statistical mechanics and thermodynamics, we show that an adiabatically driven deformation may not only increase the peak phase-space density, but also lower the temperature and spin-polarize the atoms.

The model

We consider a surface trap, where the atoms are bound to a potential of the form $U(x)+U_L(y)+U_h(z)$, where x, y, and z are Cartesian coordinates. The dependence on z is assumed to be harmonic, $U_h(z) = Mw_0^2z^2/2$, with w_0 being the trapping frequency in the direction perpendicular to the surface. In the x and y directions, the atoms are confined to a slab of length l and width L. We set $U_L(y) \equiv 0$ in the interval $0 < y < L$, and choose for $U(x)$ a square potential of height Π and width ηl ($\eta < 1$) sitting on a constant-valued potential extending over the interval $0 < x < l$. Overall, the potential inside the slab reads $U_t(x, y, z) = Mw_0^2z^2/2+U(x)$. Figure 9 shows the trap boundaries and the potential $U_t(x, y, z)$ in a plane (x, z) at a fixed value of y. This simple model for the trap can produce rather realistic results for the generic case when a potential is modified by an amount Π in a fraction η of the trap volume.

Starting by writing the canonical partition function Z_N for an ensemble of N identical atoms in the potential described above, we derive the Helmholtz free en-

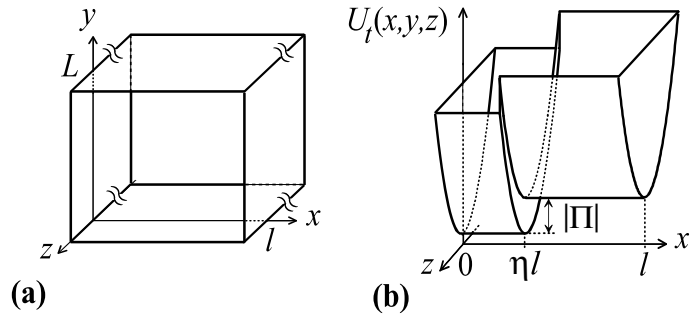

Figure 9: (a) The trap boundaries in the x and y directions. (b) The trapping potential, $U_t(x, y, z)$, in a plane (x, z) at a fixed y from the interval $0 < y < L$. In the sketch, Π is negative.

ergy $F = -k_B T \ln Z_N$ and the entropy $S = -\partial F/\partial T$. The chemical potential is found as $\mu = \partial F/\partial N$. For the stepwise shape of $U(x)$, we then obtain the following analytical expressions for the one-particle dimensionless entropy $s = S/Nk_B$, and for the mean energy per particle $\epsilon = (F+TS)/Nk_B$ and the chemical potential $\xi = \mu/k_B$, both expressed in units of temperature,

$$s = 3 - \ln \frac{\Phi(T)}{1-\eta+\eta e^{-\Delta/T}} + \frac{\eta e^{-\Delta/T}\Delta}{T(1-\eta+\eta e^{-\Delta/T})}, \tag{46}$$

$$\epsilon = \epsilon_0 + 2T + \frac{\eta e^{-\Delta/T}\Delta}{1-\eta+\eta e^{-\Delta/T}}, \tag{47}$$

$$\xi = \epsilon_0 + T \ln \frac{\Phi(T)}{1-\eta+\eta e^{-\Delta/T}}. \tag{48}$$

Here $\Delta = \Pi/k_B$ is the local change of the potential and ϵ_0 the potential at the bottom of the non-deformed trap, both again given in units of temperature. The peak phase-space density $\Phi(T)$ in the non-deformed trap and the corresponding density $n(T)$ are found as

$$\Phi(T) = \frac{2\pi\hbar^3 w_0 N}{k_B^2 T^2 M l L}, \tag{49}$$

$$n(T) = \sqrt{\frac{M}{2\pi k_B T}}\,\frac{w_0 N}{lL}. \tag{50}$$

The phase-space density $\Phi(T, \Delta, \eta)$ at the potential minimum within the deformation and the corresponding density $n(T, \Delta, \eta)$ can then be obtained from

$$\Phi(T, \Delta, \eta) = \frac{\Phi(T)}{\eta + (1-\eta)e^{\Delta/T}}, \text{and} \tag{51}$$

$$n(T, \Delta, \eta) = \frac{n(T)}{\eta + (1-\eta)e^{\Delta/T}}. \tag{52}$$

In the case of a single atomic species in the trap, an adiabatic change of the potential is characterized by

$$s(T_i, \Delta_i, \eta_i) = s(T_f, \Delta_f, \eta_f)\,, \tag{53}$$

which states the requirement for conservation of entropy. The indices i and f denote the initial and final values of the variables, respectively. By solving Eq. (53), one can find T_f, and subsequently, all the other thermodynamic parameters of the system.

If then two or more atomic species k, each in thermal equilibrium in their own locally deformed potential well, are allowed to exchange energy but not particles, the final equilibrium temperature T_f of the whole system can be calculated by equating the initial and final total energies of the system. On the other hand, if the deformations are varied adiabatically starting from a common temperature, the final temperature is found by equating the entropy of the whole system before and after the transformation,

$$\sum_k s_k(T_i, \Delta_{ki}, \eta_{ki}) N_k = \sum_k s_k(T_f, \Delta_{kf}, \eta_{kf}) N_k\,. \tag{54}$$

Next we think of atoms in a particular quantum state as a species that *can* exchange particles with the other species. We start by considering the case when each species is initially in its own equilibrium at a temperature T_{ki}, whereafter the exchanges of energy and particles equilibrate the whole system. Since the system as a whole is closed, the total energy is conserved, i.e.,

$$\sum_k \epsilon_k(T_{ki}, \Delta_k, \eta_k) N_{ki} = \sum_k \epsilon_k(T_f, \Delta_k, \eta_k) N_{kf}\,. \tag{55}$$

The final state will contain species with equal chemical potentials. Thus, we have

$$\xi_k(T_f, \Delta_k, \eta_k) = \xi_{k'}(T_f, \Delta_{k'}, \eta_{k'})\,, \tag{56}$$

$$\sum_k N_{kf} = N\,, \tag{57}$$

where k and k' denote different species, and N is the conserved total number of atoms. The final temperature T_f and the atom numbers for each species, N_{kf}, are found by solving Eqs. (55)-(57).

Yet another situation can occur, if the local deformations of the states evolve adiabatically in an already equilibrated system. Then the chemical potentials of the subensembles will be equal at each moment of the transformation and the entropy of the whole system will be conserved. Hence, the equations for T_f and N_{kf} are

$$\xi_k(T_f, \Delta_{kf}, \eta_{kf}) = \xi_{k'}(T_f, \Delta_{k'f}, \eta_{k'f}), \tag{58}$$

$$\sum_k N_{kf} = N_t, \tag{59}$$

$$\sum_k s_k(T_i, \Delta_{ki}, \eta_{ki}, N_{ki}) N_{ki} = \sum_k s_k(T_f, \Delta_{kf}, \eta_{kf}, N_{kf}) N_{kf}. \tag{60}$$

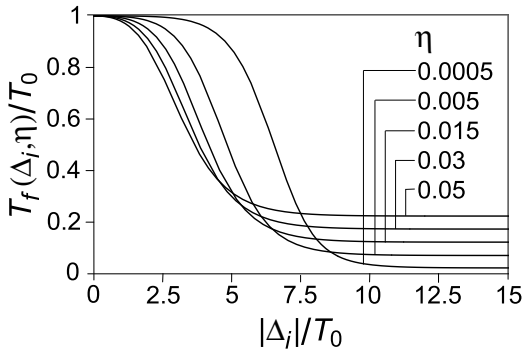

Figure 10: Decrease of temperature in an atom trap caused by the adiabatic removal of a subtrap.

This simple model can be exploited to calculate T_f and N_{kf} in the processes considered above. In order to match requirements of a different situation, where atoms still experience a slowly varying deformation of the confining potential, one can develop an analogous theoretical model by making use of classical statistical mechanics and applying a corresponding conservation law of thermodynamics.

Applications

We first consider the possibility to reach a lower temperature in laser cooling by introducing a small potential well in the trap during the cooling stage and then adiabatically removing the well after the cooling is complete. This method can be applied, if the cooling efficiency does not change in the presence of the subtrap and if the cooled sample can reach thermal equilibrium before the cooling mechanisms are switched off. These conditions can be satisfied in the evanescent-wave cooling of atoms in a GOST [97, 99, 105, 108, 120]. Figure 10 shows the final temperature, $T_f(\Delta_i, \eta)$, that can be achieved by using a subtrap of initial depth $|\Delta_i|$ ($\Delta_i < 0$) and an effective volume characterized by η. The calculations are done with the aid of Eq. (53), where Δ_f is set to 0 and both η_i and η_f are replaced with the same parameter η. For generality, we use the dimensionless variables η and $|\Delta_i|/T_0$, where T_0 is the initial temperature [$T_0 \equiv T_i \equiv T_f(\Delta_i = 0)$]. The calculations show that after cooling of the atoms in the presence of a small subtrap, the temperature may be decreased by an additional order of magnitude by slowly switching the subtrap off. The dependence of $T_f(\Delta_i, \eta)/T_0$ on the relative size of the subtrap can be explained as follows. When the subtrap is slowly removed, each atom initially confined in the subtrap converts a part of its kinetic energy into the potential energy determined by the initial depth of the subtrap. Thus, at small $|\Delta_i|/T_0$, the method works better with a larger subtrap, since it initially holds more atoms. When $|\Delta_i|/T_0$ is increased, more atoms turn out to be transferred into the subtrap in the course of

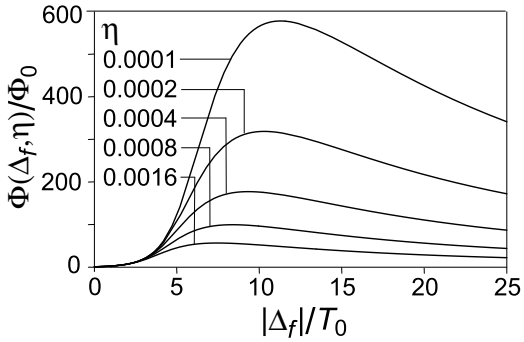

Figure 11: Increase of the peak phase-space density of trapped atoms caused by adiabatic insertion of a subtrap.

cooling. Then, at a certain value of $|\Delta_i|/T_0$, a majority of the atoms end up to be in the subtrap. In this case, a smaller subtrap is superior. We should note, however, that it is not always possible to create such a deep and small subtrap. Moreover, tight confinement can lead to an inappropriate increase of the loss rates due to inelastic interatomic collisions. Therefore, optimal values for the parameters η and $|\Delta_i|/T_0$ should be chosen depending on the particular experimental conditions. Once the parameters are selected, Fig. 10 can be used to evaluate the expected temperature.

In the next example we calculate the peak phase-space density of atoms in a trap with an adiabatically inserted subtrap [143]. This density, $\Phi(\Delta_f, \eta)$, normalized to its original value $\Phi_0 = \Phi(\Delta_f = 0)$ is shown in Fig. 11 as a function of $|\Delta_f|/T_0$, the final depth of the subtrap over the initial temperature, for a few values of η, the volume ratio. The calculations are carried out using Eq. (53) with $\Delta_i = 0$ and $\eta_i = \eta_f \equiv \eta$ to find T_f, and Eq. (51) to find $\Phi(T_f, \Delta_f, \eta) \equiv \Phi(\Delta_f, \eta)$. The results agree well with the experiments of Ref. [108], where the phase-space density was locally increased by two orders of magnitude by using a "dimple" trap within a GOST. It is important to note that when applying a deep and small subtrap, the factor by which the phase-space density increases is essentially independent of whether the insertion of the subtrap is adiabatic or not. Abruptly turning on a microscopic electro-optical atom trap, as discussed in section 4.2, will result in a local increase of the phase-space density by the same order of magnitude. Thus, in order to roughly assess the phase-space density in a tight and deep subtrap, one can directly use Eqs. (41) and (42).

Figure 11 shows that at each fixed value of η, there is an optimum value of $|\Delta_f|/T_0$, at which the phase-space density reaches its maximum. Above this value, the number of atoms transferred into the subtrap becomes too large, so that the rest of the atoms in the trap can no longer keep the temperature at the same low level.

Still another example introduces the case when a spin-independent atom trap is locally deformed with a magnetic field. In a dipole trap containing, e.g., spin-

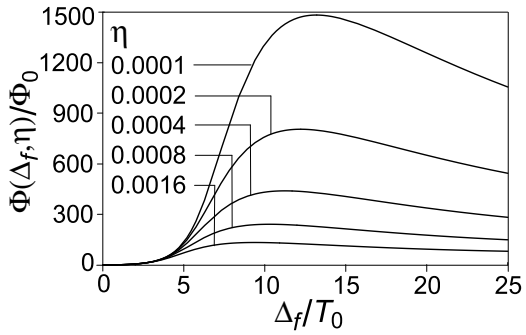

Figure 12: Increase of the peak phase-space density of atoms in a particular magnetic state due to adiabatic deformation of the trap with a static magnetic field.

unpolarized ^{87}Rb atoms in the lower hyperfine ground state, the magnetic field splits up the sample into three species characterized by the magnetic quantum numbers $m_F = \{-1, 0, +1\}$. When the trap is deformed with a locally high magnetic field (see the trap in Fig. 8a of section 4.2), the atoms with $m_F = +1$ are attracted to the deformation, while atoms with $m_F = -1$ are repelled from it. The deformation can also be created by using a magnetic-field minimum, which will attract the $m_F = -1$ atoms (see the trap in Fig. 8b). Independently of the deformation type, there will be three species ($k = 1, 2, 3$) which initially had $\Delta_{ki} = 0$ and after the deformation $\Delta_{kf} = \{-\Delta_f, 0, +\Delta_f\}$, where now Δ_f is chosen to be positive. All the parameters η_{ki} stay at their initial values which are the same for all the species, $\eta_{kf} \equiv \eta$.

Let us denote the initial temperature by T_0, and the initial phase-space density, which is equal for all the species, by Φ_0. We calculate the enhancement of the phase-space density, $\Phi(T_f, -\Delta_f, \eta)/\Phi_0$, for the species with $\Delta_{kf} = -\Delta_f$, considering three different cases. In the *first case* we assume that the exchange of energy between the species occurs much faster than particle exchange, and ignore the latter altogether. We simply apply the conservation of entropy in Eq. (54). In the *second case*, we allow the equilibration of atom numbers to follow the equilibration of temperature. We solve Eq. (54), and then replace all T_{ki} in Eqs. (55) and (56) with the obtained T_f. Then, by solving Eqs. (55)-(57), we find new values for T_f and the atom numbers N_{kf}. In the *third case* we allow the system to be in total equilibrium (thermal and chemical) at each moment of the transformation, and use Eqs. (58)-(60) directly. When the phase-space density increases substantially for the species attracted toward the deformation, $\Phi(T_f, -\Delta_f, \eta) \gg \Phi_0$, the results for the three scenarios turn out to be almost indistinguishable. In Fig. 12 we show a plot corresponding to the first case. The dependence of $\Phi(T_f, -\Delta_f, \eta)/\Phi_0$ on the parameters η and Δ_f/T_0 is similar to the dependence illustrated in Fig. 11 for a single species. However, here the factor by which the phase-space density increases

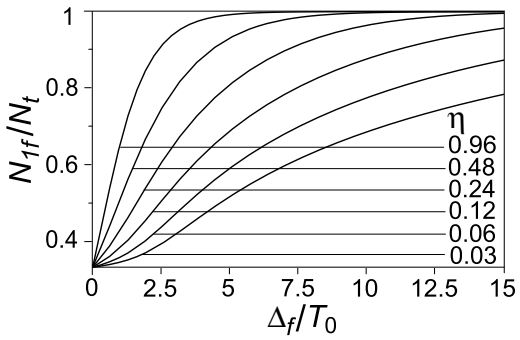

Figure 13: Spin polarization of atoms in a dipole trap due to adiabatic deformation of the trapping potential with a static magnetic field.

is about three times larger, as if the sample was spin-polarized at the temperature T_0 prior to applying the magnetic field. This is exactly the effect discussed in the second subsection of section 4.2, where loading of atoms into a surface-mounted magnetic microtrap is discussed.

Our final example describes a method to spin-polarize atoms without increasing the temperature. Let atoms in a ground state with three magnetic substates be stored in a dipole trap in the presence of an external magnetic field. The magnetic field splits the initial degeneracy of the species by moving apart the magnetic energy levels by an amount larger than $k_B T_0$. However, if an rf field tuned into resonance with the splitting is used to accelerate the equilibration between the species, the degeneracy is restored as far as thermodynamics is concerned. Next, a local magnetic-field deformation is inserted adiabatically. The final atom numbers N_{kf} of the three magnetic states can be found by solving Eqs. (58)-(60) with $\eta_{ki} = \eta_{kf} \equiv \eta$, $\Delta_{ki} = 0$, and $\Delta_{kf} = \{-\Delta_f, 0, +\Delta_f\}$. The dependence of the normalized population N_{1f}/N_t ($k = 1$ corresponds to the state deformed by $-\Delta_f$) on η and Δ_f/T_0 is plotted in Fig. 13. The result shows that the use of a deformation with a large relative volume, η, and/or a large relative strength, Δ_f/T_0, can provide nearly complete spin polarization of the atoms. By switching off the rf field and slowly removing the deformation, one can then return the trap to its initial shape and the sample to its initial temperature, but with the atoms occupying a single magnetic substate. We note that decoupling of the magnetic states by switching off the rf field leads to an essential change of the system, because the rest of the transformation proceeds without equilibration of the magnetic-state populations. The disappearance of the rf field does not affect the spatial profiles of the magnetic energy levels and, therefore, the temperature at this stage remains unchanged.

The above examples show that by allowing transitions between the Zeeman states of the atoms in conjunction with adjustments of the shape of the atom trap, flexibility can be added to the preparation of an atomic sample in a microtrap that

can be part of an “atom chip” [60]. Such an atom chip could be made on a transparent substrate and contain not only magnetic microtraps, but also static electric and all-optical traps. A gravito-optical surface trap could then serve as an initial source of atoms and as the trap to be locally modified.

5 Summary and discussions

In this thesis, we have described certain general aspects of trapping and cooling of neutral atoms on an evanescent optical wave. In particular, we have investigated the influence of multiple reabsorption of resonance-frequency photons in an evanescent-wave cooled atom sample on the final temperature and phase-space density. We found that, if the atoms are subjected to an on-resonance repumping, the final temperature becomes an increasing function of the number of atoms, while the phase-space density shows a well-established maximum. After passing this maximum, the phase-space density starts to decrease due to heating of the atoms by spontaneously emitted photons which are multiply reabsorbed in the sample before escaping from it. The results of this study have a straightforward practical application. If, for example, the loss rate of atoms within the cooling stage is known, one can achieve a maximum possible phase-space density by selecting the initial number of atoms to be larger than the optimum number by a fraction expected to be lost during the cooling. The maximum possible value of the phase-space density can in turn be increased by reducing the trap size or, alternatively, by using a repumper which is not based on spontaneous emission following resonance excitation of the atoms.

As regards of realization of a steep ring-shaped potential barrier for the lateral confinement of atoms on an evanescent-wave mirror, the thesis introduces a simple optical system, consisting of a nematic liquid crystal and two lenses, which is able to produce a thin-walled hollow laser beam of tunable cross-sectional dimension and peak intensity. This optical system may be employed not only in trapping and guiding of atoms, but also in manipulation of microscopic objects and in material testing.

In the thesis, we have described several basic designs of surface-mounted microscopic atom traps built on an optically transparent substrate. The transparency of the substrate enables unimpeded control of the external and internal degrees of freedom of atoms with laser light. In particular, loading of atoms into the microtrap can be realized by making use of a gravito-optical surface trap. We have described here a loading technique based on local phase-space compression, which allows the phase-space density in the microtrap to exceed the level of 10^{-2}. This value is several orders of magnitude higher than the one typically achieved in loading of conventional traps on current-carrying wires. When loading a magnetic microtrap with atoms, initial spin polarization of the sample as a way to increase the phase-space density is not necessary. We showed that, independently of whether the insertion of the microtrap into the GOST is adiabatic or not, the phase-space density reaches essentially the same level as if the sample was originally spin-polarized. This is explained by the fact that the “wrong-polarized” atoms contribute to the local phase-space density of the trapped-state atoms through retaining the temperature

of the “heat bath”.

Besides a purely magnetic trap for low-field seeking atoms, the method we have put forward allows realizing a low-field seeker trap combined with a repulsive evanescent wave. In contrast to the traditional traps where the Majorana spin flips are prevented by applying a magnetic field in the direction parallel to the wire, the trap on an evanescent-wave mirror does not require such a field component. Thus, by using paired wires with co-directed currents one can completely remove the necessity of an external magnetic field and create atom guides with essentially arbitrary in-plane geometry. A high-field seeker trap, also introduced in the thesis, provides the same opportunity without doubling the wires. In addition, such a trap can store atoms in their most stable true ground state.

If a magneto-optical or pure magnetic trap is created on a selectively magnetized thin film made of a high-coercivity iron garnet, the magnetic-field fluctuations become significantly reduced. It would also be possible to erase a former magnetization pattern on the film and record a new one, which will conveniently allow the same device to be used for testing different trap configurations.

In the thesis, we have also described the basic principles of a microscopic electro-optical trap. This trap can store both unpolarized atom samples and samples polarized into a particular magnetic state. Using the electro-optical trap, one can magnetically tune the interactions between the atoms without affecting the confining potential. In contrast to an all-optical microtrap created in a GOST by a vertical infrared laser beam [99, 108], our trap can be designed to tightly confine atoms in all three directions or to serve as an atom guide with micrometer-scale transverse dimensions.

In order to investigate the possibilities to manipulate atomic states by making use of an adiabatically driven local deformation of the trapping potential, we have proposed a simple, but rather generic theoretical model which is based on classical statistical mechanics and thermodynamics. Providing the possibility to describe multi-species atom samples, the model allows for different responses of the species to a deformation and for both thermal and chemical equilibration. We have demonstrated how a local deformation of the confining potential may decrease the temperature, increase the phase-space density of atoms in a particular magnetic state, and spin-polarize the atoms in an initially spin-independent trap without increase in the temperature.

Experimental verification of these proposals is currently in progress in our laboratory. In particular, the construction of equipment to demonstrate trapping of ^{87}Rb in a low-field seeker microtrap on a selectively magnetized iron-garnet thin film is in the final stages and repeated writing of magnetization patterns has already been achieved. In the future, this trapping technique may be used for creation of Bose-Einstein condensates and for realization of a gas of “impenetrable bosons”. We believe that the rewritable permanent-magnet patterns on a metal-free transparent

substrate will provide an extra flexibility and stability for the experiments.

References

[1] I. I. Rabi, J. R. Zacharias, S. Millman, P. Kusch, *Phys. Rev.* **53**, 318 (1938).

[2] N. F. Ramsey, *Phys. Rev.* **76**, 996 (1949).

[3] Ye. V. Baklanov, B. Ya. Dubetsky, V. P. Chebotayev, *Appl. Phys.* **9**, 171 (1976).

[4] C. R. Bordé, *C. J. Acad. Sci. Ser. B* **248**, 101 (1977).

[5] A. Ashkin, *Phys. Rev. Lett.* **25**, 1321 (1970).

[6] R. Schieder, H. Walter, L. Wöste, *Opt. Commun.* **5**, 337 (1972).

[7] J.-L. Picque, J.-L. Vialle, *Opt. Commun.* **5**, 402 (1972).

[8] R. J. Cook, A. F. Bernhardt, *Phys. Rev. A* **18**, 2533 (1978).

[9] E. Arimondo, H. Lew, T. Oka, *Phys. Rev. Lett.* **43**, 753 (1979).

[10] A. P. Kazantsev, *Sov. Phys. JETP* **36**, 861 (1973).

[11] A. Ashkin, *Phys. Rev. Lett.* **24**, 156 (1970).

[12] A. Ashkin, *Phys. Rev. Lett.* **40**, 729 (1978).

[13] T. W. Hänsch, *Opt. Commun.* **13**, 68 (1975).

[14] V. S. Letokhov, V. G. Minogin, B. D. Pavlik, *Opt. Commun.* **19**, 72 (1976).

[15] S. Stenholm, J. Javanainen, *Appl. Phys.* **16**, 159 (1978).

[16] V. I. Balykin, V. S. Letokhov, V. I. Mushin, *JETP lett.* **29**, 560 (1979).

[17] E. L. Raab, M. Prentiss, A. Cable, S. Chu, D. E. Pritchard, *Phys. Rev. Lett.* **59**, 2631 (1987).

[18] H. F. Hees, *Phys. Rev. B* **34**, 3476 (1986).

[19] M. H. Anderson, J. R. Ensher, M. R. Matthews, C. E. Wieman, E. A. Cornell, *Science* **269**, 198 (1995).

[20] K. Davis, M.-O. Mewes, M. Andrews, M. van Druten, D. Durfee, D. Kurn, W. Ketterle, *Phys. Rev. Lett.* **75**, 3969 (1995).

[21] C. C. Bradley, C. A. Sackett, J. J. Tollett, R. G. Hulet, *Phys. Rev. Lett.* **75**, 1687 (1995).

[22] D. Fried, T. Killian, L. Willmann, D. Landhuis, S. Moss, D. Kleppner, T. Greytak, *Phys. Rev. Lett.* **81**, 3811 (1998).

[23] S. Cornish, N. Claussen, J. Roberts, E. Cornell, C. Wieman, *Phys. Rev. Lett.* **85**, 1795 (2000).

[24] G. Modugno, G. Ferrari, G. Roati, R. J. Brecha, A. Simoni, M. Inguscio, *Science* **294**, 1320 (2001).

[25] A. Robert, O. Sirjean, A. Browaeys, J. Poupard, S. Nowak, D. Boiron, C. I. Westbrook, A. Aspect, *Science* **292**, 461 (2001).

[26] T. Weber, J. Herbig, M. Mark, H.-C. Nägerl, R. Grimm, *Science* **299**, 232 (2003).

[27] M. W. Zwierlein, C. A. Stan, C. H. Schunck, S. M. F. Raupach, S. Gupta, Z. Hadzibabic, W. Ketterle, *Phys. Rev. Lett.* **91**, 250401 (2003).

[28] S. Jochim, M. Bartenstein, A. Altmeyer, G. Hendl, S. Riedl, C. Chin, J. H. Denschlag, R. Grimm, *Science* **302**, 2101 (2003).

[29] M. Greiner, C. A. Regal, D. S. Jin, *Nature* **426** 537 (2003).

[30] C. Raman, M. Köhl, R. Onofrio, D. S. Durfee, C. E. Kuklewicz, Z. Hadzibabic, W. Ketterle, *Phys. Rev. Lett.* **83**, 2502 (1999).

[31] R. Onofrio, C. Raman, J. M. Vogels, J. R. Abo-Shaeer, A. P. Chikkatur, W. Ketterle, *Phys. Rev. Lett.* **85**, 2228 (2000).

[32] S. Burger, F. S. Cataliotti, C. Fort, F. Minardi, M. Inguscio, M. L. Chiofalo, M. P. Tosi, *Phys. Rev. Lett.* **86**, 4447 (2001).

[33] D. Guéry-Odelin, S. Stringari, *Phys. Rev. Lett.* **83**, 4452 (1999).

[34] O. M. Maragó, S. A. Hopkins, J. Arlt, E. Hodby, G. Hechenblaikner, C. J. Foot, *Phys. Rev. Lett.* **84**, 2056 (2000).

[35] M. Greiner, O. Mandel, T. Esslinger, T. W. Hänsch, I. Bloch, *Nature* **415**, 39 (2002).

[36] D. L. Feder, M. S. Pindzola, L. A. Collins, B. I. Schneider, C. W. Clark, *Phys. Rev. A* **62**, 053606 (2002).

[37] Z. Dutton, M. Budde, C. Stowe, L. V. Hau, *Science* **293**, 663 (2001).

[38] M. R. Matthews, B. P. Anderson, P. C. Haljan, D. S. Hall, C. E. Wieman, E. A. Cornell, *Phys. Rev. Lett.* **83**, 2498 (1999).

[39] K. W. Madison, F. Chevy, W. Wohlleben, J. Dalibard, *Phys. Rev. Lett.* **84**, 806 (2000).

[40] J. R. Abo-Shaeer, C. Raman, J. M. Vogels, W. Ketterle, *Science* **292**, 476 (2001).

[41] E. Hodby, G. Hechenblaikner, S. A. Hopkins, O. M. Maragó, C. J. Foot, *Phys. Rev. Lett.* **88**, 010405 (2002).

[42] G. Lens, P. Meystre, E. W. Wright, *Phys. Rev. Lett.* **71**, 3271 (1993).

[43] M. Trippenbach, Y. B. Band, P. S. Julienne, *Opt. Express* **3**, 530 (1998).

[44] S. Inouye, A. P. Chikkatur, D. M. Stamper-Kurn, J. Stenger, D. E. Pritchard, W. Ketterle, *Science* **285**, 571 (1999).

[45] M. Kozuma, Y. Suzuki, Y. Torii, T. Sugiura, T. Kuga, E. W. Hagley, L. Deng, *Science* **286**, 2309 (1999).

[46] S. Inouye, T. Pfau, S. Gupta, A. P. Chikkatur, A. Görlitz, D. E. Pritchard, W. Ketterle, *Nature* **402**, 641 (1999).

[47] M.-O. Mewes, M. R. Andrews, D. M. Kurn, D. S. Durfee, C. G. Townsend, W. Ketterle, *Phys. Rev. Lett.* **78**, 582 (1997).

[48] I. Bloch, T. W. Hänsch, T. Esslinger, *Phys. Rev. Lett.* **82**, 3008 (1999).

[49] E. W. Hagley, L. Deng, M. Kozuma, J. Wen, K. Helmerson, S. L. Rolston, W. D. Phillips, *Science* **283**, 1706 (1999).

[50] K. M. O'Hara, S. L. Hemmer, M. E. Gehm, S. R. Granade, J. E. Thomas, *Science* **298**, 2179 (2002).

[51] H. Dieckman, C. A. Stan, S. Gupta, Z. Hadzibabic, S. Schunck, W. Ketterle, *Phys. Rev. Lett.* **89**, 203201 (2002).

[52] Z. Hadzibabic, S. Gupta, C. A. Stan, C. H. Schunck, M. W. Zwierlein, K. Dieckman, W. Ketterle, *Phys. Rev. Lett.* **91**, 160401 (2003).

[53] J. Cubizolles, T. Bourdel, S. J. J. M. F. Kokkelmans, G. V. Shlyapnikov, C. Salomon, *Phys. Rev. Lett.* **91**, 240401 (2003).

[54] M. Bartenstein, A. Altmeyer, S. Riedl, S. Jochim, C. Chin, J. H. Denschlag, R. Grimm, *Phys. Rev. Lett.* **92**, 120401 (2004).

[55] M. Bartenstein, A. Altmeyer, S. Riedl, S. Jochim, C. Chin, J. H. Denschlag, R. Grimm, *Phys. Rev. Lett.* **92**, 203201 (2004).

[56] C. A. Regal, C. Ticknor, J. L. Bohn, D. S. Jin, *Nature* **424**, 47 (2003).

[57] G. Modugno, F. Ferlaino, R. Heidemann, G. Roati, M. Inguscio *Phys. Rev. A* **68**, 011601 (2003).

[58] E. Tiesinga, B. J. Verhaar, H. T. C. Stoof, *Phys. Rev. A* **47**, 4144 (1993).

[59] S. Inouye, M. R. Andrews, J. Stenger, H.-J. Miesner, D. M. Stamper-Kurn, W. Ketterle, *Nature* **392**, 151 (1998).

[60] R. Folman, P. Krüger, J. Schmiedmayer, J. Denschlag, and C. Henkel, *Adv. At. Mol. Phys.* **48**, 263 (2002).

[61] J. Reichel, *Appl. Phys. B* **75**, 469 (2002).

[62] D. Cassettari, A. Chenet, R. Folman, A. Haase, B. Hessmo, P. Krüger, T. Maier, S. Schneider, T. Calarco, J. Schmiedmayer, *Appl. Phys. B* **70**, 721 (2000).

[63] M. Vengalattore, W. Rooijakkers, M. Prentiss, *Phys. Rev. A* **66**, 053403 (2002).

[64] P. Krüger, X. Luo, M. W. Klein, K. Brugger, A. Haase, S. Wildermuth, S. Groth, I. Bar-Joseph, R. Folman, J. Schmiedmayer, *Phys. Rev. Lett.* **91**, 233201 (2003).

[65] S. K. Sekatskii, B. Riedo, G. Dietler, *Opt. Commun.* **195**, 197 (2001).

[66] W. Hänsel, P. Hommelhoff, T. W. Hänsch, J. Reichel, *Nature* **413**, 498 (2001).

[67] S. Schneider, A. Kasper, Ch. vom Hagen, M. Bartenstein, B. Engeser, T. Schumm, I. Bar-Joseph, R. Folman, L. Feenstra, J. Schmiedmayer, *Phys. Rev. A* **67**, 023612 (2003).

[68] R. Folman, P. Krüger, D. Cassettari, B. Hessmo, T. Maier, J. Schmiedmayer, *Phys. Rev. Lett.* **84**, 4749 (2000).

[69] J. Reichel, W. Hänsel, P. Hommelhoff, T. W. Hänsch, *Appl. Phys. B* **72**, 81 (2001).

[70] J. Schmiedmayer, *Eur. Phys. J. B* **4**, 57 (1998).

[71] N. H. Dekker, C. S. Lee, V. Lorent, J. H. Thywissen, S. P. Smith, M. Drndic, R. M. Westervelt, M. Prentiss, *Phys. Rev. Lett.* **84**, 1124 (2000).

[72] D. Cassettari, B. Hessmo, R. Folman, T. Maier, J. Schmiedmayer, *Phys. Rev. Lett.* **85**, 5483 (2000).

[73] D. Müller, E. A. Cornell, M. Prevedelli, P. D. D. Schwindt, A. Zozulya, D. Z. Anderson, *Opt. Lett.* **25**, 1382 (2000).

[74] E. A. Hinds, C. J. Vale, M. G. Boshier, *Phys. Rev. Lett.* **86**, 1462 (2001)

[75] W. Hänsel, J. Reichel, P. Hommelhoff, T. W. Hänsch, *Phys. Rev. A* **64**, 063607 (2001).

[76] E. Andersson, T. Calarco, R. Folman, M. Andersson, B. Hessmo, J. Schmiedmayer, *Phys. Rev. Lett.* **88**, 100401 (2002)

[77] M. Vengalattore, W. Rooijakkers, M. Prentiss, *Phys. Rev. A* **66**, 53403 (2002).

[78] W. Rooijakkers, W. Saijun, P. Striehl, M. Vengalattore, M. Prentiss, *Phys. Rev. A* **68**, 63412 (2003).

[79] M. Vengalattore, R. S. Conroy, W. Rooijakkers, M. Prentiss, *J. Appl. Phys.* **95**, 4404 (2004).

[80] G. Birkl, F. B. J. Buchkremer, R. Dumke, W. Ertmer, *Opt. Commun.* **191**, 67 (2001).

[81] R. Dumke, M. Volk, T. Muther, F. B. J. Buchkremer, G. Birkl, W. Ertmer, *Phys. Rev. Lett.* **89**, 097903(2002).

[82] R. Dumke, T. Muther, M. Volk, W. Ertmer, G. Birkl, *Phys. Rev. Lett.* **89**, 220402(2002).

[83] C. Henkel, S. Pötting, M. Wilkens, *Appl. Phys. B* **69**, 379 (1999).

[84] C. Henkel, P. Krüger, R. Folman, J. Schmiedmayer, *Appl. Phys. B* **76** 173 (2003).

[85] E. Andersson, S. M. Barnett, *Phys. Rev. A* **62**, 052311 (2000).

[86] J. H. Thywissen, M. Olshanii, G. Zabow, M. Drndic, K. S. Johnson, R. M. Westervelt, M. Prentiss, *Eur. Phys. J. D* **7**, 361 (1999).

[87] A. Imamoglu, M. Lewenstein, L. You, *Phys. Rev. Lett.* **78**, 2511 (1997).

[88] D. S. Petrov, G. V. Shlyapnikov, J. T. M. Walraven, *Phys. Rev. Lett.* **87**, 050404 (2001).

[89] S. Dettmer, D. Hellweg, P. Ryytty, J. J. Arlt, W. Ertmer, K. Sengstock, D. S. Petrov, G. V. Shlyapnikov, H. Kreutzmann, L. Santos, and M. Lewenstein, *Phys. Rev. Lett.* **87**, 160406 (2001).

[90] A. Görlitz, J. M. Vogels, A. E. Leanhardt, C. Raman, T. L. Gustavson, J. R. Abo-Shaeer, A. P. Chikkatur, S. Gupta, S. Inouye, T. Rosenband, W. Ketterle, *Phys. Rev. Lett.* **87**, 130402 (2001).

[91] M. Olshanii, *Phys. Rev. Lett.* **81**, 938 (1998).

[92] K. K. Das, M. D. Girardeau, E. M. Wright, *Phys. Rev. Lett.* **89**, 170404 (2002).

[93] J. I. Cirac, P. Zoller, H. J. Kimble, H. Mabuchi, *Phys. Rev. Lett.* **78**, 3221 (1997).

[94] H. Mabuchi, A. C. Doherty, *Science* **298**, 1372 (2002).

[95] T. Calarco, E. A. Hinds, D. Jaksch, J. Schmiedmayer, J. I. Cirac, P. Zoller, *Phys. Rev. A* **61**, 022304 (2000).

[96] Yu. B. Ovchinnikov, I. Manek, R. Grimm, *Phys. Rev. Lett.* **79** 2225 (1997).

[97] M. Hammes, D. Rychtarik, V. Druzhinina, U. Moslener, I. Manek-Hönninger, R. Grimm, *J. Mod. Opt.* **47**, 2755 (2000).

[98] I. Manek, Yu. B. Ovchinnikov, R. Grimm, *Opt. Commun.* **147**, 67 (1998).

[99] D. Rychtarik, B. Engeser, H.-C. Nägel, R. Grimm, Phys. *Rev. Lett.* **92**, 173003 (2004).

[100] J. Schmiedmayer, *Eur. Phys. J. D* **4**, 57 (1998).

[101] J. Schmiedmayer, *Appl. Phys. B* **60**, 169 (1995).

[102] I. I. Rabi, *Phys. Rev.* **51**, 625 (1937).

[103] H. J. Metcalf, P. van der Straten, *Laser Cooling and Trapping* (Springer-Verlag New York, Inc., New York, 1999).

[104] B. W. Shore, *The theory of coherent atomic excitation* (John Wiley & Sons, Inc., New York, 1990).

[105] J. Söding, R. Grimm, Yu. B. Ovchinnikov, *Opt. Commun.* **119**, 652 (1995).

[106] P. Desbiolles, M. Arndt, P. Szriftgiser, J. Dalibard, *Phys. Rev. A* **54**, 4292 (1996).

[107] R. J. C. Spreeuw, D. Voigt, B. T. Wolschrijn, H. B. van Linden den Heuvell, *Phys. Rev. A* **61**, 053604 (2000).

[108] M. Hammes, D. Rychtarik, H.-C. Nägel, R. Grimm, *Phys. Rev. A* **66**, 051401 (2002).

[109] M. Hammes, D. Rychtarik, B. Engeser, H.-C. Nägel, R. Grimm, *Phys. Rev. Lett.* **90**, 173001 (2003).

[110] H. Gauck, M. Hartl, D. Schneble, H. Schnitzler, T. Pfau, J. Mlynek, *Phys. Rev. Lett.* **81**, 5298 (1998).

[111] P. Domokos, H. Ritsch, *Europhys. Lett.* **54**, 306 (2001).

[112] M. Gorliki, S. Feron, V. Lorent, and M. Ducloy, *Phys. Rev. A* **61**, 013603 (2000).

[113] C. Henkel, K. Mølmer, R. Kaiser, N. Vansteenkiste, C. I. Westbrook, A. Aspect, *Phys. Rev. A* **55**, 1160 (1997).

[114] V. Savalli, D. Stevens, J. Estève, P. D. Featonby, V. Josse, N. Westbrook, C. I. Westbrook, A. Aspect, *Phys. Rev. Lett* **88**, 250404 (1997).

[115] S. Marksteiner, C. M. Savage, P. Zoller, S. L. Rolston, *Phys. Rev. A* **50**, 2680 (1993).

[116] D. J. Harris, C. M. Savage, *Phys. Rev. A* **51**, 3967 (1995).

[117] H. Ito, K. Sakaki, T. Nakata, W. Jhe, M. Ohtsu, *Optics Comm.* **115**, 57 (1995).

[118] M. J. Renn, E. A. Donley, E. A. Cornell, C. E. Wieman, D. Z. Anderson, *Phys. Rev. A* **53**, R648 (1996).

[119] D. Müller, E. A. Cornell, D. Z. Anderson, E. R. I. Abraham, *Phys. Rev. A* **61**, 033411 (2000).

[120] Yu. B. Ovchinnikov, I. Manek, R. Grimm, *Phys. Rev. Lett.* **79**, 2225 (1997).

[121] M. Hammes, D. Rychtarik, V. Druzhinina, U. Moslener, I. Manek-Hönninger, R. Grimm, *J. Mod. Opt.* **47**, 2755 (2000).

[122] M. V. Subbotin, V. I. Balykin, D. V. Laryushin, V. S. Letokhov, *Opt. Commun.* **139**, 107 (1997).

[123] H. Nha, W. Jhe, *Phys. Rev. A* **56**, 729 (1997).

[124] J. Yin, Y. Zhu, Y. Wang, *Phys. Lett. A* **248**, 309 (1998).

[125] Y. Song, D. Milam, W. T. Hill III, *Opt. Lett.* 24, 1805 (1999).

[126] J. Arlt, R. Kuhn, K. Dholakia, *J. Mod. Opt.* **48** 783 (2001).

[127] S. Nowak, N. Stuhler, T. Pfau, J. Mlynek, *Phys. Rev. Lett.* **81**, 5792 (1998).

[128] J. Denschlag, G. Umshaus, J. Schmiedmayer, *Phys. Rev. Lett.* **81**, 737 (1998).

[129] J. Denschlag, J. Schmiedmayer, *Europhys. Lett.* **6**, 405 (1997).

[130] J. Schmiedmayer, *Phys. Rev. A* **52**, R13 (1995).

[131] J. Denschlag, D. Cassettari, J. Schmiedmayer, *Phys. Rev. Lett.* **82**, 2014 (1999).

[132] V. Vuletic, T. W. Hänsch, C. Zimmermann, *Europhys. Lett.* **36**, 349 (1996).

[133] J. Reichel, W. Hänsel, T. W. Hänsch, *Phys. Rev. Lett.* **83**, 3398 (1999).

[134] S. Schneider, A. Kasper, Ch. vom Hagen, M. Bartenstein, B. Engeser, T. Schumm, I. Bar-Joseph, R. Folman, L. Feenstra, J. Schmiedmayer, *Phys. Rev. A* **67**, 023612 (2003).

[135] H. Ott, J. Fortagh, G. Schlotterbeck, A. Grossmann, C. Zimmermann, *Phys. Rev. Lett.* **87**, 230401 (2001).

[136] T. L. Gustavson, A. P. Chikkatur, A. E. Leanhardt, A. Görlitz, S. Gupta, D. E. Pritchard, W. Ketterle, *Phys. Rev. Lett.* **88**, 020401 (2002).

[137] E. D. Palik, *Handbook of Optical Constants of Solids* (Academic Press, New York, 1998).

[138] R. Marani, L. Cognet, V. Savalli, N. Westbrook, C. I. Westbrook, A. Aspect, *Phys. Rev. A* **61**, 053402 (2000).

[139] Y. Colombe, D. Kadio, M. Olshanii, B. Mercier, V. Lorent, H. Perrin, *J. Opt. B: Quantum Semiclass. Opt.* **5**, S155 (2003).

[140] S. D. Gensemer, V. Sanchez-Villicana, K. Y. N. Tan, T. T. Grove, P. L. Gould, *Phys. Rev. A* **56**, 4055 (1997).

[141] A. J. Moerdijk, H. M. J. M. Boesten, B. J. Verhaar, *Phys. Rev. A* **53**, 619 (1996).

[142] P. W. H. Pinkse, A. Mosk, M. Weidemüller, M. W. Reynolds, T. W. Hijmans, J. T. M. Walraven, *Phys. Rev. Lett.* **78**, 990 (1997).

[143] D. M. Stamper-Kurn, H.-J. Miesner, A. P. Chikkatur, S. Inouye, J. Stenger, W. Ketterle, *Phys. Rev. Lett.* **81**, 2194 (1998).

[144] L. Viverit, S. Giorgini, L. P. Pitaevskii, S. Stringari, *Phys. Rev. A* **63**, 033603 (2001).

[145] A. E. Leanhardt, A. P. Chikkatur, D. Kielpinski, Y. Shin, T. L. Gustavson, W. Ketterle, D. E. Pritchard, *Phys. Rev. Lett.* **89**, 040401 (2002).

Abstracts of Publications I-V

I. We present a simple method to convert a Gaussian laser beam into an annular beam using a homeotropically oriented nematic liquid crystal. The method allows creation of a beam with sub-millimeter diameter and a width of a few tens of μm for a propagation distance of more than 10 mm. High spatial gradients in the radial intensity distribution make the beams promising for use in atom trapping and guiding.

II. We show that multiple reabsorption of resonance-frequency photons in a cloud of evanescent-wave cooled atoms can have a significant influence on the cooling efficiency and maximum value of the atomic phase-space density.

III. We put forward the idea of a surface-mounted microscopic electro-optical atom trap. The trap is formed on an evanescent-wave atom mirror by the strongly localized static electric field of two oppositely charged transparent electrodes placed close to each other. The electrodes are embedded in a refractive-index-matched thin dielectric layer on the surface of a glass prism. In our example, the phase-space density in the trap center reaches 0.1, when the trap is loaded with atoms from a gravito-optical surface trap.

IV. We describe a method for obtaining a high phase-space density of alkali atoms in a surface-mounted microscopic atom trap created above a transparent conductor or permanent magnet on a substrate prism. We show that the peak value of the phase-space density can locally reach the level of $\sim 10^{-2}$ when the microtrap is loaded with atoms from a gravito-optical surface trap. Initial spin polarization of the atoms is not required.

V. We use classical statistical mechanics and thermodynamics to describe the response of a trapped multi-species atomic sample to a local deformation in the confining potential. An adiabatic deformation may not only increase the peak phase-space density, but also lower the temperature and spin-polarize the atoms.